Secondary $PM_{2.5}$ decreases significantly less than NO_2 emission reductions during COVID lockdown in Germany

Vigneshkumar Balamurugan[1], Jia Chen[1], Zhen Qu[2], Xiao Bi[1], and Frank N. Keutsch[2,3]

[1]Environmental Sensing and Modeling, Technical University of Munich (TUM), Munich, Germany
[2]School of Engineering and Applied Science, Harvard University, Cambridge, MA, USA
[3]Department of Chemistry and Chemical Biology, Harvard University, Cambridge, MA, USA

Correspondence: Vigneshkumar Balamurugan (vigneshkumar.balamurugan@tum.de), Jia Chen (jia.chen@tum.de)

Abstract. This study estimates the influence of anthropogenic emission reductions on the concentration of particulate matter with a diameter smaller than 2.5 μm ($PM_{2.5}$) during the 2020 lockdown period in German metropolitan areas. After accounting for meteorological effects, $PM_{2.5}$ concentrations during the spring 2020 lockdown period were 5 % lower compared to the same time period in 2019. However, during the 2020 pre-lockdown period (winter), meteorology accounted for $PM_{2.5}$ concentrations were 19 % lower than in 2019. Meanwhile, meteorology accounted for NO_2 concentrations dropped by 23 % during the 2020 lockdown period compared to an only 9 % drop for the 2020 pre-lockdown period, both compared to 2019. Meteorology accounted for SO_2 and CO concentrations show no significant changes during the 2020 lockdown period compared to 2019. GEOS-Chem (GC) simulation with a COVID-19 emission reduction scenario based on the observations (23 % reduction in anthropogenic NO_X emission with unchanged anthropogenic VOC and SO_2) are consistent with the small reductions of $PM_{2.5}$ during the lockdown and are used to identify the underlying drivers for this. Due to being in a NO_X saturated ozone production regime, GC OH radical and O_3 concentrations increased (15 and 9 %, respectively) during the lockdown compared to a Business As Usual (no lockdown) scenario. O_X (=NO_2+O_3) analysis implies that the increase in ozone at night-time is solely due to reduced NO titration. The increased O_3 results in increased NO_3 radical concentrations, primarily during the night, despite the large reductions in NO_2. Thus, the oxidative capacity of the atmosphere is increased in all three important oxidants, OH, O_3, and NO_3. PM nitrate formation from gas-phase nitric acid (HNO_3) is decreased during the lockdown as the increased OH concentration cannot compensate for the strong reductions in NO_2 resulting in decreased day-time HNO_3 formation from the OH + NO_2 reaction. However, night-time formation of PM nitrate from N_2O_5 hydrolysis is relatively unchanged. This results from the fact that increased night-time O_3 results in significantly increased NO_3 which roughly balances the effect of the strong NO_2 reductions on N_2O_5 formation. Ultimately, the only small observed decrease in lockdown $PM_{2.5}$ concentrations can be explained by the large contribution of night-time PM nitrate formation, generally enhanced sulfate formation and slightly decreased ammonium. This study also suggests that high $PM_{2.5}$ episodes in early spring are linked to high atmospheric ammonia concentrations combined with favorable meteorological conditions of low temperature and low boundary layer height. North-West Germany is a hot-spot of NH_3 emissions, primarily emitted from livestock farming and intensive agricultural activities (fertilizer application), with high NH_3 concentrations in the early spring and summer months. Based on our findings, we suggest that appropriate NO_X and VOC emission controls are required to limit ozone, and that should also

help reduce PM$_{2.5}$. Regulation of NH$_3$ emissions, primarily from agricultural sectors, could result in significant reductions in PM$_{2.5}$ pollution.

1 Introduction

To halt the spread of the COVID-19 virus, various strict measures such as social isolation, curfews, and travel restrictions were implemented around the world in early 2020 (Steinmetz et al., 2020). As a result of these restrictions, anthropogenic emissions decreased significantly (Schumann et al., 2021; Le Quéré et al., 2020; Turner et al., 2020). Reduced primary emission activities from road transportation and industrial activities were expected to improve air quality. Numerous studies using satellite and in-situ measurements have reported significant reductions in primary air pollutant concentrations during the COVID-19 lockdown period compared to pre-lockdown period in various parts of the world (Bauwens et al., 2020; Biswal et al., 2020; Collivignarelli et al., 2020; Dietrich et al., 2021; Field et al., 2020; He et al., 2021; Pathakoti et al., 2020; Mendez-Espinosa et al., 2020), but also emphasize the importance of accounting for the effects of different meteorological conditions between the study period and the reference period (Barré et al., 2020; Grange et al., 2020; Kroll et al., 2020; Koukouli et al., 2021; Ordóñez et al., 2020; Solberg et al., 2021). Anomalies in air pollutant concentrations caused by changes in meteorological conditions were also separated from observed changes using modeling work to estimate the actual influence of COVID-19 lockdown restrictions on air pollutant concentration changes (Balamurugan et al., 2021; Goldberg et al., 2020; Kang et al., 2020; Petetin et al., 2020; Qu et al., 2021; Yin et al., 2021). Secondary pollutant concentrations (O$_3$ and PM$_{2.5}$), which are primarily produced by precursor gases through complex atmospheric chemical reactions, remarkably increased or did not reduce commensurate to precursor emission reductions seen in some parts of the world during the COVID-19 lockdown period (Campbell et al., 2021; Deroubaix et al., 2021; He et al., 2021; Huang et al., 2021; Keller et al., 2021; Lee et al., 2020; Putaud et al., 2021; Souri et al., 2021; Wang et al., 2020, 2021).

Particulate Matter (PM) is the sum of all particles (solid and liquid) suspended in air, and can be classified based on aerodynamic behavior, i.e., aerodynamic diameter (AD). Particles with an AD smaller than 10 μm are referred to as PM$_{10}$, while particles smaller than 2.5 μm AD are referred to as PM$_{2.5}$. Understanding of seasonal and inter-annual variability of PM, particularly over urban areas, remains a challenge (Fuzzi et al., 2015). This is mainly due to a lack of understanding in the attribution of PM sources. PM sources include both direct/primary sources (vehicle and industrial emissions, wind-blown dust, pollen, wildfires, etc.) as well as secondary formation (gas-to-particle conversion process) via atmospheric chemical reaction of precursor compounds such as NO$_X$ (nitrogen oxides), SO$_2$ (sulfur dioxide), NH$_3$ (ammonia), VOCs (Volatile Organic Compounds) and other organic compounds, including compounds that have partitioned from primary aerosol back to the gas-phase, followed by partitioning to the condensed phase (Allen et al., 2015; Ayres et al., 2015; Fisher et al., 2016; Hallquist et al., 2009; Jacob, 1999; Jacobson, 1999; Marais et al., 2016; Seinfeld and Pankow, 2003; Steinfeld, 1998; Zhang et al., 2015). The composition of PM thus varies greatly depending on time and location; for example, in urban areas nitrate and organic aerosol often dominate in winter time ~~Cesari et al., 2018; Zhai et al., 2021~~ (Cesari et al., 2018; Juda-Rezler et al., 2020; Samek et al., 2020; Salameh et al., 2015; Womack et al., 2019; Zhai et al., 2021).

In this study, we mainly focus on the response of urban surface $PM_{2.5}$ to COVID-19 lockdown restrictions in Germany. Because major anthropogenic emissions are reduced, this unplanned intervention can test the understanding of the contribution of secondary $PM_{2.5}$ sources, as well as the processes important in secondary $PM_{2.5}$ formation. Despite of significant reductions in some anthropogenic activities, natural and agricultural air pollutant sources were not affected by the COVID-19 lockdown measures. Ammonia (NH_3) emissions (agricultural sources) are a significant source of $PM_{2.5}$ in Germany in the spring (Fortems-Cheiney et al., 2016), when lockdown restrictions are implemented. Secondary inorganic aerosols such as ammonium sulfate and ammonium nitrate are the largest contributors to $PM_{2.5}$ in Europe (Pay et al., 2012; Petetin et al., 2016). In comparison to sulfate formation, nitrate formation is more dependent on NH_3 concentration (Erisman and Schaap, 2004; Sharma et al., 2007; Wu et al., 2008). In the winter and spring (low temperature and high relative humidity), the role of NH_3 in $PM_{2.5}$ formation is greater than in the summer (high temperature and low relative humidity) (Schiferl et al., 2016; Squizzato et al., 2013; Viatte et al., 2020). Primary components of $PM_{2.5}$ are directly proportional to primary emission but secondary components of $PM_{2.5}$ are not directly proportional to secondary precursor emissions or concentrations as they are produced by non-linear complex atmospheric chemical reactions (Shah et al., 2018). Observational and modeling evidence is required to estimate the influence of change in precursor emissions on $PM_{2.5}$ concentrations. To this end, we used ground and space-based measurements of $PM_{2.5}$, NO_2, O_3, SO_2, CO and NH_3 in conjunction with GEOS-Chem simulations to investigate the influence of lockdown restrictions on $PM_{2.5}$ concentrations.

Modelling studies such as Gaubert et al. (2021); Hammer et al. (2021); Matthias et al. (2021); Menut et al. (2020) have already reported the $PM_{2.5}$ changes across Europe including Germany, during the COVID-19 lockdown period. The activity data (e.g., transportation, industrial activities and energy production) were used in the above mentioned studies to create a COVID-19 emission reduction scenario (Doumbia et al., 2021; Guevara et al., 2021). However, there are large discrepancies between various activity data sets (Gensheimer et al., 2021), necessitating different approaches to estimating the actual emission reduction caused by the COVID-19 lockdown restrictions. In this study, GEOS-Chem simulations (using identical anthropogenic emission for 2020 and 2019) were used to estimate the meteorology accounted for observed pollutant concentrations changes between 2020 and 2019, which were then used as a proxy for emissions reductions caused by COVID-19 lockdown measures to create a COVID-19 emission scenario in GEOS-Chem model for simulating the lockdown pollutant concentrations (Fig. 1). In addition to looking at the impact of lockdown restrictions on air pollutant concentrations (Sect. 4.1), we focus on process level analysis of the impact of changes in precursor emissions (NO_X) on $PM_{2.5}$ formation (Sect. 4.2), as well as the role of ammonia (NH_3) emissions in $PM_{2.5}$ formation (Sect. 4.3).

2 Data and Model

Data sets used in this study are summarized in Table 1. We focused on ten metropolitan areas in Germany (Bremen, Cologne, Dresden, Dusseldorf, Frankfurt, Hamburg, Hanover, Leipzig, Munich and Stuttgart) and used surface air pollutant concentration data ($PM_{2.5}$, NO_2, O_3) for all of these while SO_2 data was only available for five of these areas (Bremen, Dresden, Frankfurt, Hamburg and Leipzig) and CO data was limited to six metropolitan areas (Bremen, Frankfurt, Hamburg, Hanover, Munich

Table 1. Data sets used in this study.

Data source	Data	Temporal resolution	Spatial resolution	Data availability
Governmental in-situ measurements	NO_2, O_3, $PM_{2.5}$	1 h	-	Bremen, Cologne, Dresden, Dusseldorf, Frankfurt, Hamburg, Hanover, Leipzig, Munich and Stuttgart metropolitan areas
	SO_2	1 h	-	Bremen, Dresden, Frankfurt, Hamburg and Leipzig metropolitan areas
	CO	1 h	-	Bremen, Frankfurt, Hamburg, Hanover, Munich and Stuttgart metropolitan areas
TROPOMI satellite measurements	SO_2	daily	7*3.5 km (5.5*3.5 km, after August 6, 2019)	All of Germany
IASI satellite measurements	NH_3	twice a day	12 km diameter	All of Germany
		monthly	1 degree	All of Germany
ERA 5 (ECMWF reanalysis)	Temperature, relative humidity, boundary layer height and wind speed	1 h	0.25 degree	All of Germany
	Precipitation	daily	1 degree	All of Germany
GEOS-Chem (GC) chemical transport model	All species	1 h	0.5 * 0.625 degree	All of Germany

and Stuttgart). We use data for 2019 and 2020 in this work (data-obtained from https://discomap.eea.europa.eu/map/fme/AirQualityExport.htm).

TROPOMI tropospheric SO_2 (Theys et al., 2017) column products are also used (offline products-obtained from https://s5phub.copernicus.eu). The TROPOMI SO_2 product provides the total SO_2 column between the surface and the top of tropo-
95 sphere. The TROPOMI overpass occurs around 13.30 local time. At the start of the mission, the TROPOMI product provided data at a resolution of 7*3.5 km, while after August 6, 2019 the resolution improved to 5.5*3.5 km. Stricter quality filtering criteria (quality assurance value (qa) >= 0.5) was applied to the dataset. A daily mean of SO_2 is calculated by averaging these values within 0.5-degree radius of the urban center.

100 The daily atmospheric NH_3 variability in Germany was studied using the "near-real time daily IASI/Metop-B ammonia (NH3) total column (ANNI-NH3-v3)" dataset (products-obtained from https://iasi.aeris-data.fr/catalog/). The data used are from the IASI instrument aboard the Metop-B satellite, which has a local solar overpass time of 9:30 a.m and 9:30 p.m (Clerbaux et al., 2009). We only used day-time (9.30 am) measurements in this study. Night-time measurements (9.30 pm) were excluded due to their large relative errors. A daily mean is calculated by averaging the values within 0.5-degree radius of
105 the urban center. The monthly atmospheric NH_3 variability in Germany was studied using the "standard monthly IASI/Metop-B ULB-LATMOS ammonia (NH3) L3 product (total column)" dataset. This product contains a monthly averaged NH_3 total column with a spatial resolution of 1*1 degree (products-obtained from https://iasi.aeris-data.fr/catalog/).

Temperature, relative humidity, boundary layer height and wind information are obtained from the ERA 5 product (Hersbach et al., 2020). This product's native spatial and temporal resolutions are 0.25 degree and 1 hour, respectively. For precipitation
110 information, the GPCP daily gridded product from ERA 5 is used, which provides global gridded data at 1-degree resolution (products-obtained from https://cds.climate.copernicus.eu/).

We used the GEOS-Chem (GC) chemical transport model (http://doi.org/10.5281/zenodo.3959279) to simulate the pollutant concentration for 2020 and 2019. The GC simulation conducted over Germany (4-17°E, 45-57°N) had a horizontal resolution

of 0.5°*0.625° with dynamic boundary conditions generated from a global simulation with 4°*5° resolution. We ran the GC simulation for two cases. In the first case, anthropogenic emissions from the 2014 CEDS inventory (Hoesly et al., 2018), the most recent version of which is 2014, are used in the GC simulations for both 2019 and 2020, but with the corresponding meteorology from MERRA-2 global reanalysis product for 2019 and 2020. Natural emissions from soil and lightning are calculated for the corresponding year using mechanisms described in Hudman et al. (2012) and Murray (2016). The corresponding year's open fire emissions from GFED4 (Werf et al., 2017) are used for 2019 and 2020. In the second case, the 2014 CEDS anthropogenic emission inventory were scaled down by the estimated emissions reduction caused by the lockdown restrictions for the 2020 lockdown period. The remaining (natural and fire) emissions are calculated in the same way as in the first case. Even though the 2014 CEDS anthropogenic emission inventory is used in GC simulations, the effects of anthropogenic emission changes between 2014 and 2019 or 2020 will be canceled out because we use the difference between two years (e.g., 2020 - 2019) or two cases (e.g., $2020_{lockdown}$ - $2020_{no\ lockdown}$) in our study.

3 Method

The following is our methodology for estimating meteorology accounted for observed pollutant concentration changes between 2020 and 2019, similar to Balamurugan et al. (2021); Qu et al. (2021). We estimate the difference in pollutant concentrations between 2020 and 2019 caused by changes in meteorology using GC simulated concentrations (first case). Since GC uses identical anthropogenic emission for 2020 and 2019, with the corresponding year meteorology, the difference between 2020 and 2019 GC pollutant (e.g., $PM_{2.5}$) concentrations only results from meteorology changes between 2020 and 2019. We use Δ to signify absolute concentration change, and f to signify fractional (percentage) change.

$$\Delta PM_{2.5(GC)} = PM_{2.5(GC,2020)} - PM_{2.5(GC,2019)} \tag{1}$$

The observed (ground-truth measurements) pollutant concentration changes between 2020 and 2019, which includes the effects of lockdown restrictions and meteorology, is:

$$\Delta PM_{2.5(obs)} = PM_{2.5(obs,2020)} - PM_{2.5(obs,2019)} \tag{2}$$

To disentangle the meteorology contribution from the observed pollutant concentration changes, we subtract the GC pollutant concentration changes caused by meteorology from observed pollutant concentration changes between 2020 and 2019.

$$\Delta PM_{2.5(obs,emi)} = \Delta PM_{2.5(obs)} - \Delta PM_{2.5(GC)} \tag{3}$$

The fractional change in meteorology accounted for pollutant concentration between 2020 and 2019, i.e. ~~pollutant concentration changes between 2020 and 2019 due to emission changes only~~ fractional change (%) in pollutant concentration between 2020 and 2019 due to emission changes only, is calculated as,

$$fPM_{2.5(obs,emi)} = \frac{\Delta PM_{2.5(obs,emi)}}{PM_{2.5(obs,2019)}} * 100 \tag{4}$$
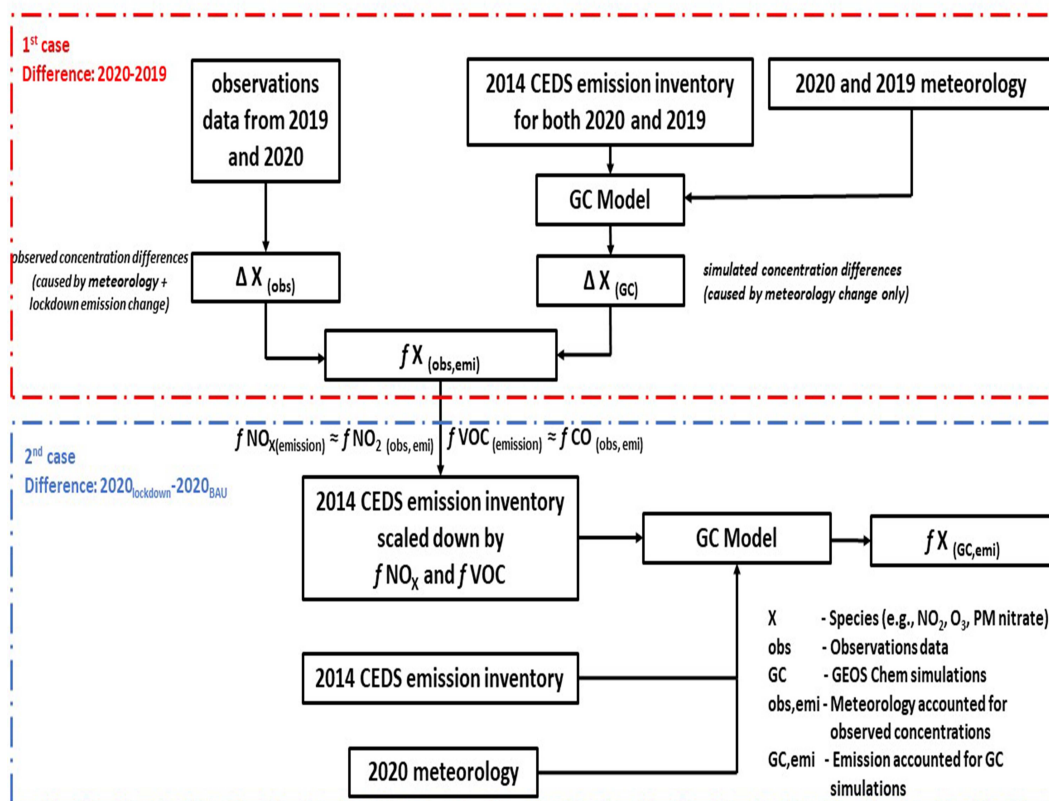
Figure 1. Schematic diagram of our methodology for calculating the meteorology accounted for observed pollutant concentrations changes between 2020 and 2019, and emission accounted for GC pollutant concentrations changes between 2020 lockdown and 2020 BAU scenario.

where, "obs", "GC" and "obs,emi" refer to ground-truth measurements (observations data), GEOS-Chem simulations and meteorology accounted for ground-truth measurements, respectively.

145   We estimate the meteorology accounted for fractional change in other pollutant concentrations analogously. Our previous study (Balamurugan et al., 2021), using the same methodology, reported the meteorology accounted for NO_2 and O_3 concentration changes for eight German metropolitan areas. Here, we reproduce the results for NO_2 and O_3 concentrations, but for ten metropolitan areas. We use $fNO_{2(obs,emi)}$ and $fCO_{(obs,emi)}$ to capture fractional changes in anthropogenic NO_X and VOC emission ($fNO_{X(emission)}$) and $fVOC_{(emission)}$)) due to lock down restrictions, respectively. Because of the scarcity of VOC

150   measurements, CO data was used as a proxy for anthropogenic VOC (Fujita et al., 2003; Jiménez et al., 2005; Stephens et al., 2008; Yarwood et al., 2003) and NO_2 was used as proxy for NO_X. This assumption is supported by studies such as Baker et al. (2008); Von Schneidemesser et al. (2010), which show anthropogenic VOC is well correlated with CO, and Blanchard and Tanenbaum (2003), which shows comparable changes in VOC and CO between weekday and weekend. Changes in biogenic

VOCs are not directly affected by lockdown measures.

$$fNO_{X(emission)} \approx fNO_{2(obs,emi)} \tag{5}$$

$$fVOC_{(emission)} \approx fCO_{(obs,emi)} \tag{6}$$

The base anthropogenic emission inventory were then scaled down by $fNO_{X(emission)}$ and $fVOC_{(emission)}$ for NO_X and VOC emission, respectively, in the GC model for the 2020 lockdown period (second case), which simulates all pollutants concentrations for the lockdown emission scenario. The fractional change in emission accounted for, i.e. using scaled emission inventories, GC pollutants level during the 2020 lockdown period compared to 2020 Business As Usual (BAU), i.e., no lockdown, level is calculated as,

$$fPM_{2.5(GC,emi)} = \frac{PM_{2.5(GC,2020,lock)} - PM_{2.5(GC,2020)}}{PM_{2.5(GC,2020)}} * 100 \tag{7}$$

where, "GC,emi" refers to GC simulations accounting for scaled emission and $PM_{2.5(GC,2020,lock)}$ are the $PM_{2.5}$ concentrations during the lockdown period determined via the 2020 GC simulations with down-scaled emissions. We estimate the emission accounted for concentration changes of other pollutants in the same way. Figure 1 illustrates our methodology for calculating the meteorology accounted for observed pollutant concentrations changes between 2020 and 2019, as well as emission accounted for GC pollutant concentration changes between 2020 lockdown and 2020 BAU scenario.

4 Results and discussion

4.1 Influence of lockdown restrictions on the concentrations of air pollutants

To assess the impact of lockdown restrictions on the concentration of air pollutants, we compared the 2020 lockdown period pollutant concentrations to the same period in 2019. These comparison results, however, need to take the effects of both meteorological and lockdown restrictions into account. As mentioned in Sect. 3, we used GEOS-Chem simulations to disentangle the effects of meteorology on observed pollutant concentration changes between 2020 and 2019. Studies such as Balamurugan et al. (2021) and Tai et al. (2012) have shown that GEOS-Chem can reproduce the temporal variability of observed pollutant concentrations including $PM_{2.5}$, emphasizing that GC can be used for process level analysis of $PM_{2.5}$ variability. We also compared the 2019 GC and 2019 observed in-situ $PM_{2.5}$ concentrations and found that the GC and observed in-situ $PM_{2.5}$ concentrations were in good agreement (R > 0.5 for all metropolitan areas, except Leipzig which has a R value of 0.39) ~~(e.g., Fig. 6 (c), for Cologne metropolitan area)~~. Table A1 shows the statistical evaluation (R, RMSE and mean bias) of the GC model performance for each metropolitan area. The GC simulations underestimate the $PM_{2.5}$ when compared to observed in-situ $PM_{2.5}$ concentrations (mean bias ((GC - in-situ)/in-situ) ranges from -12.7 % to -37.4 %), except for the Cologne metropolitan area (+ 11.7 %). However, since we use the GC's relative difference between 2020 and 2019, this bias should cancel out. We also compared the 2019 GC simulated nitrate and ammonium concentration for the urban measurement station in Germany (14.33°E,
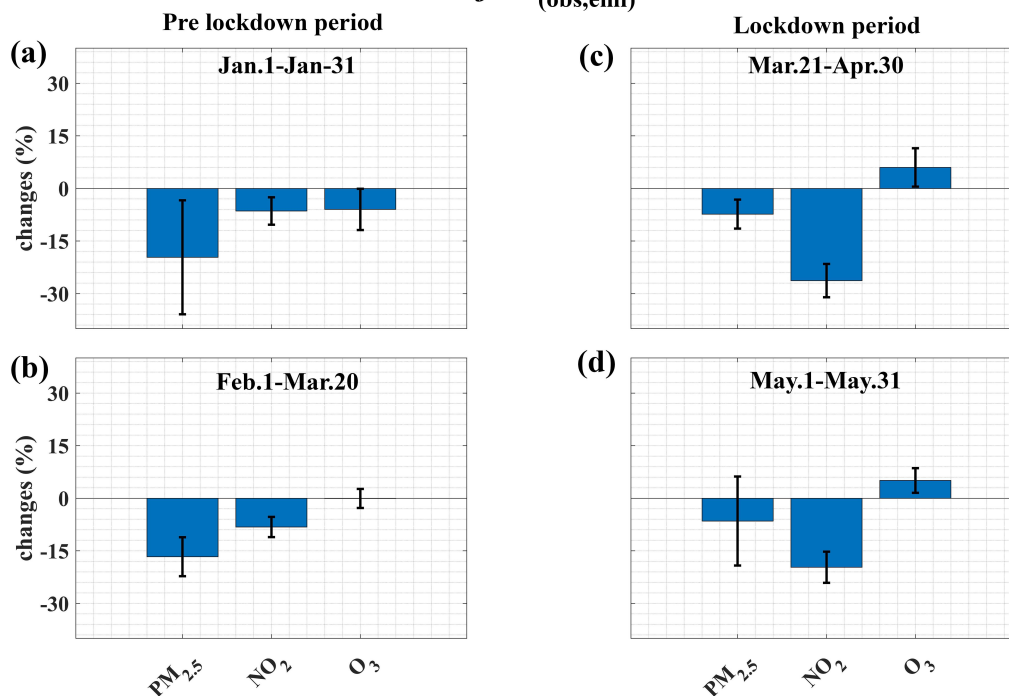
Figure 2. Meteorology accounted for mean in-situ $PM_{2.5}$, NO_2, and O_3 concentration changes between 2020 and 2019. Results of computations according to our first case ($fX_{(obs,emi)}$) in the Sect. 3. Error bars represent the 1σ of mean of ten metropolitan areas.

51.75°N). The statistical evaluation (R, RMSE and mean bias) of the GC model performance for these species is given in Table
185 B1.

Figure 2 shows meteorology accounted for mean $PM_{2.5}$, NO_2 and O_3 concentration changes between 2020 and 2019 for ten German metropolitan areas from January 1 through May 31. Both meteorology accounted and unaccounted for mean $PM_{2.5}$, NO_2 and O_3 concentration changes between 2020 and 2019 for ten German metropolitan areas are shown in Appendix Fig. A1. The German government imposed COVID-19 lockdown restrictions on March 21, 2020 in Germany. In figures and
190 for specific cases, the pre-lockdown period (January 1 to March 20) is divided into two sections, and the lockdown period (March 21 to May 31) is also divided into two sections (unless otherwise specified): (a) January 1 to January 31, 2020 - No lockdown restrictions, (b) February 1 to March 20, 2020 - No lockdown restrictions in the event of unusual weather conditions (occurrence of storms), (c) March 21 to April 30, 2020 (spring) - Strict lockdown measures, and (d) May 1 to May 31, 2020 (late spring) - Loose lockdown measures. Germany experienced high wind conditions due to storms in February 2020 (Matthias
195 et al., 2021), which was used to determine the extent of meteorology's role in pollutant concentration changes. Meteorology unaccounted for mean NO_2 and $PM_{2.5}$ concentrations for February 1 to March 20, 2020 period (before the implementation of lockdown) are lower than the corresponding ones in 2019 by 30 % and 42 % ($fNO_{2(obs)}$ and $fPM_{2.5(obs)}$), respectively, due to

the dilution/dispersion from the high wind conditions. However, after accounting for meteorology, the difference in mean NO_2 and $PM_{2.5}$ concentrations between 2020 and 2019 for the period February 1 to March 20 ($fNO_{2(obs,emi)}$ and $fPM_{2.5(obs,emi)}$) are 8 % and 18 %, respectively. This finding is consistent with meteorology accounted for mean NO_2 and $PM_{2.5}$ changes between 2020 and 2019 for the period January 1 to January 31 (Fig. 2 (a,b)). This highlights the importance of accounting for meteorological impacts.

In the 2020 pre-lockdown period (January 1 to March 20), both meteorology accounted for mean NO_2 and $PM_{2.5}$ levels are lower by 9 % and 19 %, respectively, compared to the same period in 2019. During the 2020 lockdown period (March 21 to May 31), mean meteorology accounted for NO_2 concentrations dropped significantly (23 %) compared to the same period in 2019, which is greater than the drop in the 2020 pre-lockdown period compared to 2019 (9 %). Comparatively, mean meteorology accounted for 2020 lockdown $PM_{2.5}$ concentrations show a smaller reduction (5 %) compared to the same period in 2019, while an important precursor, NO_2, decreased by 23 % during the same period. Furthermore, the meteorology accounted for $PM_{2.5}$ reduction during the 2020 lockdown period (5 %) is less than the meteorology accounted for $PM_{2.5}$ reduction observed during the 2020 pre-lockdown period (19 %) compared to the corresponding 2019 periods (Fig. 2). Especially in Munich and Stuttgart, meteorology accounted for $PM_{2.5}$ concentrations during the 2020 lockdown period are higher than in 2019. The meteorology accounted for mean O_3 concentrations in the 2020 lockdown period are increased by 6 % compared to the same period in 2019. The increase in O_3 concentration during the 2020 lockdown period is mainly due to being in a NO_X saturated regime (Gaubert et al., 2021), in which reducing NO_X emission results in an increase in O_3 concentrations (Sillman, 1999; Sillman et al., 1990). It is also possible that the increase in ozone is due to less ozone destruction via lower NO titration, in addition to an increase in ozone formation efficiency through NO_X saturated regime chemistry. The meteorology accounted for mean O_X (= NO_2 + O_3) concentrations in the 2020 lockdown period is 2 % higher than in 2019 (Fig. C1(a)), implies that the reduced NO titration effect partly contributed to the increased ozone. O_X analysis also implies that the decrease in NO_2 was offset by an increase in O_3, and ozone production is overwhelmingly NO_X saturated in Germany.

The effects of lockdown restrictions on SO_2 concentrations are insignificant. In comparison to 2019, TROPOMI meteorology accounted for SO_2 levels are decreased by 1 % during the 2020 lockdown period compared to 2019 (Fig. A1). For accounting meteorological impacts on TROPOMI satellite column concentrations, GEOS-Chem diagnostics (47 vertical layers) were converted to a column, applying TROPOMI's averaging kernel. Because of the large influence of background concentration on satellite column measurements, we also investigated in-situ SO_2 concentrations, but only for five metropolitan areas. Similarly, we found that the impact of lockdown restrictions on in-situ SO_2 concentrations is marginal (Fig. B1). The road transportation sector contributes less than 1 % of total sulfur dioxide emissions, while coal-related fuel burning (industrial and energy production) accounts for nearly 80 % of total sulfur dioxide emissions (SO2, 2021). Because the lockdown restrictions primarily reduced traffic-related emissions, we see far less effects of the lockdown on SO_2 concentration (slight increase or no significant decrease in other European metropolitan areas (Collivignarelli et al., 2020; Filonchyk et al., 2021; Higham et al., 2021)). We found similar effects on in-situ CO concentration changes in six metropolitan areas. The meteorology accounted for mean CO concentrations are lower by 3 % during the 2020 lockdown period compared to 2019 (Fig. B1). Stuttgart meteorology
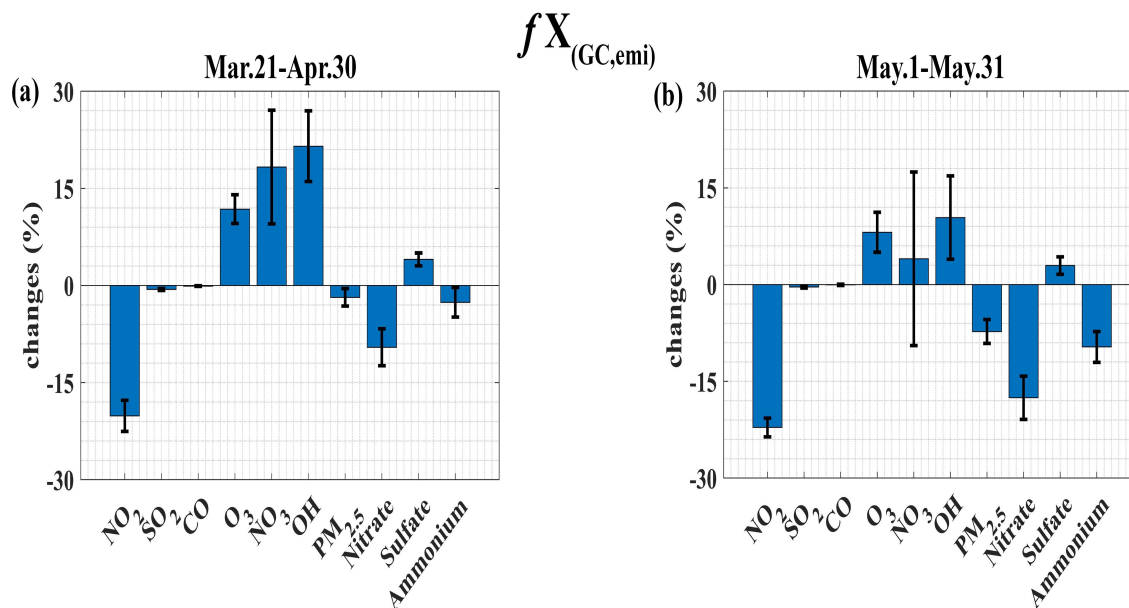
Figure 3. The emission accounted for GC NO_2, SO_2, CO, O_3, NO_3 radical, OH radical, $PM_{2.5}$, inorganic nitrate,sulfate, ammonium concentration changes between 2020 lockdown and 2020 BAU (no lockdown) scenario ($fX_{(GC,emi)}$). Error bars represent the 1 σ of mean of ten metropolitan areas.

accounted for CO concentrations in 2020 were higher than 2019 at all times. Other metropolitan areas experienced minor reductions (Clark et al., 2021; Hörmann et al., 2021).

4.2 Model evidence of changes in air pollutants concentration resulting from lockdown restrictions

235   As mentioned in Sect. 3, we use the meteorology accounted for NO_2 and CO changes to adjust the anthropogenic NO_X and VOC emissions in inventories due to lockdown restriction impacts. GC model simulations are then obtained with this scaled anthropogenic emission scenario (23 % reduction in anthropogenic NO_X emission and unchanged anthropogenic VOC emissions) for the 2020 lockdown period. The NO_X emission reduction is within the range of estimated anthropogenic NO_X emission reductions using activity data for Europe by previous authors (Doumbia et al., 2021; Guevara et al., 2021) (25 % and

240   33 %, respectively). For those studies there are large differences in estimated anthropogenic VOC emission changes for Europe; Doumbia et al. (2021) estimated 34 % while Guevara et al. (2021) estimated 8 % reduction in anthropogenic VOC emissions, compared to the BAU scenario. However, the real-time measurements at a United Kingdom station show no significant changes in many VOC concentrations during the lockdown period (Grange et al., 2020). For the NO_X saturated ozone production regime regime, VOC emission reductions can decrease ozone levels, while NO_X emission reductions increase them. Gaubert et al.

245   (2021) conducted a sensitivity study of modelling work on ozone levels in response to the NO_X or VOC or both emission reductions for the 2020 lockdown period. The reduction in both emissions (NO_X and VOC), suggested by Doumbia et al. (2021),

results in slight increase in lockdown ozone levels (< 2.5 %) over only north-western Germany and slight decrease in lockdown ozone levels over other regions of Germany, compared to BAU levels. But, only reduction in NO_X emission results in increased lockdown ozone levels (0-10 %) over all of Germany compared to BAU levels, which is also consistent with our results of increase in meteorology accounted for ozone levels over different metropolitan areas across Germany during 2020 lockdown period compared to 2019 levels. This implies that anthropogenic VOC emissions were either not reduced at all or by a much smaller percentage than anthropogenic NO_X emissions, compared to the BAU scenario. According to the European Environment Agency (EEA) (https://www.eea.europa.eu/data-and-maps/indicators/eea-32-non-methane-volatile-1/assessment-4), the road transport sector accounts for 14.6 % of total NMVOC emissions, while the road transport sector accounts for 40.5 % of total NO_X emissions (https://www.eea.europa.eu/data-and-maps/indicators/eea-32-nitrogen-oxides-nox-emissions-1/assessment.2010-08-19.0140149032-3: :text=EEA%2D33%20emissions%20of%20nitrogen,households'%20(13%25)%20sectors). According to Guevara et al. (2021), the transportation sector accounts for nearly 90 % of the reduction in total anthropogenic NO_X and VOC emissions during lockdown. As we noted that NO_X emission decreased by 23 %, and the lockdown restrictions primarily reduced traffic-related emissions, we can directly extrapolate this to a reduction in road transportation-related emissions; approximately 43 % (23-40.50 / 40.50). This finding also corresponds to a 40 % decrease in traffic vehicle count (Gensheimer et al., 2021). Therefore, the decrease in VOC emission from transport sector should be 6 % (14.6 * 0.43). However, due to a significant decline in the transport sector's VOC emission in recent years, this reduction in VOC emission from the transport sector, calculated based on the EEA's 2015 data, should be even less than 6 %. There is also no evidence that lockdown measures affect the major source of VOC emissions, which are use of volatile chemical products such as cleaning agents and personal care products, as well as biogenic emissions.

The emission accounted for GC lockdown NO_2 concentrations decreased by 21 % ($f NO_{2(GC,emi)}$) while emission accounted for GC lockdown O_3 concentrations increased by 9 % compared to 2020 BAU (Fig. 3). This is consistent with previous studies (such as Balamurugan et al. (2021); Gaubert et al. (2021)) which show that German metropolitan areas are in a NO_X saturated ozone production regime in spring. However, the diurnal cycle of GC O_X changes between 2020 lockdown and BAU suggests that night-time ozone increases are solely due to a decrease in NO titration effects (Fig. C1(b)). The emission accounted for GC lockdown PM concentrations show small decreases compared to 2020 BAU (Fig. 3). These results are consistent with previous studies (Gaubert et al., 2021; Hammer et al., 2021; Matthias et al., 2021; Menut et al., 2020), which used activity data to develop an emission reduction scenario and estimated small to no reduction in $PM_{2.5}$, a significant drop in NO_2 and marginal increase in O_3 levels during 2020 lockdown period, compared to BAU levels, over Northern-Europe including Germany.

We investigated the GC $PM_{2.5}$ composition for the studied period to determine the role of reduced NO_X emission on total $PM_{2.5}$. Major secondary $PM_{2.5}$ components are nitrate, sulfate, ammonium and organic aerosol, which, on average, correspond to 24 %, 23 %, 15 % and 30 % of total $PM_{2.5}$, respectively, during March 21 to May 31, 2019 (Fig. D1). Mean relative contribution of $PM_{2.5}$ species for 2020 (BAU) and 2020 (lockdown) are shown in Fig. E1 and F1, respectively. The emission accounted for GC PM nitrate levels during the 2020 initial lockdown period (March 21 to April 30) are 9.5 % lower than the 2020 BAU levels ($f NIT_{(GC,emi)}$) (Fig. 3 (a)), however, we see NO_2 decreased by 21 % during the same period.

The decrease in emission accounted for GC PM nitrate is also less than the decrease in NO_2 during the second half of the lockdown (May 1 to May 31). The emission accounted for GC lockdown PM sulfate level show marginal increase (3.5 %), while emission accounted for GC lockdown PM ammonium shows marginal decrease (5.8 %), compared to 2020 BAU level. The slight increase (& decrease) in sulfate (& ammonium) was also found in the Hammer et al. (2021); Matthias et al. (2021) studies, which used activity data to adjust the COVID-19 emission scenario.

It is notable that the reduction in NO_X, a precursor to PM nitrate, does not directly translated into a decrease in PM nitrate formation. There are several pathways for the formation of nitric acid (HNO_3), which partition to PM nitrate (Allen et al., 2015; Bauer et al., 2007). The reaction of OH and NO_2 (homogeneous pathway) and the hydrolysis of N_2O_5 on aerosol particles (heterogeneous pathway) are the two major pathways (Chang et al., 2011, 2016; Mollner et al., 2010).

The reaction for HNO_3 formation via gas-phase oxidation of NO_2 by OH is:

$$NO_2 + OH \xrightarrow{M} HNO_3 \tag{R1}$$
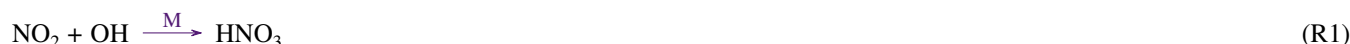
The reactions resulting in HNO_3 formation via hydrolysis of N_2O_5 on aerosol surfaces are:

$$NO_2 + O_3 \longrightarrow NO_3 + O_2 \tag{R2}$$

$$NO_3 + NO_2 \xleftarrow{M} N_2O_5 \tag{R3}$$

$$N_2O_5 + H_2O(l) \longrightarrow 2\,HNO_3 \tag{R4}$$
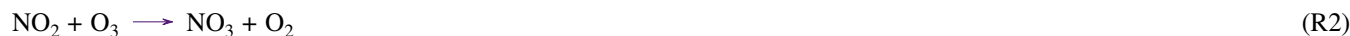
The formation of HNO_3 from the reaction of OH and NO_2 dominates during the day, while hydrolysis of N_2O_5 on aerosol particles dominates at night as OH night-time concentrations are low and N_2O_5 photolyzes easily (Russell et al., 1986). At night, NO_3 radical can be an important precursor for PM nitrate via reactions (Eq. R3, R4) (Kang et al., 2021; Shah et al., 2020; Wang et al., 2013). The emission accounted for concentrations of OH and NO_3, which drive day and night-time formation of PM nitrate, increased substantially (15 % and 12 %, respectively) during the lockdown period compared to BAU (Fig. 3). The increase in OH radicals results from German metropolitan areas being in a NO_X saturated regime (Shah et al., 2020). The increase in GC lockdown NO_3 levels is predominantly at night due to a significant increase in night-time O_3 (Fig. 4 (b,e)); the reaction of NO_2 with O_3 is the most important source of NO_3 radical (Eq. R2) (Geyer et al., 2001).

Liu et al. (2020) have demonstrated that analyzing the diurnal cycle of total inorganic nitrate helps to identify the dominant pathway for the particulate nitrate production. The emission accounted for GC lockdown PM nitrate levels decreased significantly during the day, while night-time lockdown PM nitrate levels decreased slightly compared to BAU levels (Fig. 4 (h)). Even though GC lockdown OH levels increased, HNO_3 production from the OH+NO_2 reaction during the lockdown period is reduced due to significantly lower day-time NO_2 levels compared to BAU (Fig. 4 (d)); as a result, GC day-time lockdown PM nitrate levels are significantly lower compared to BAU levels. However, higher night-time NO_3 levels result in higher night-time
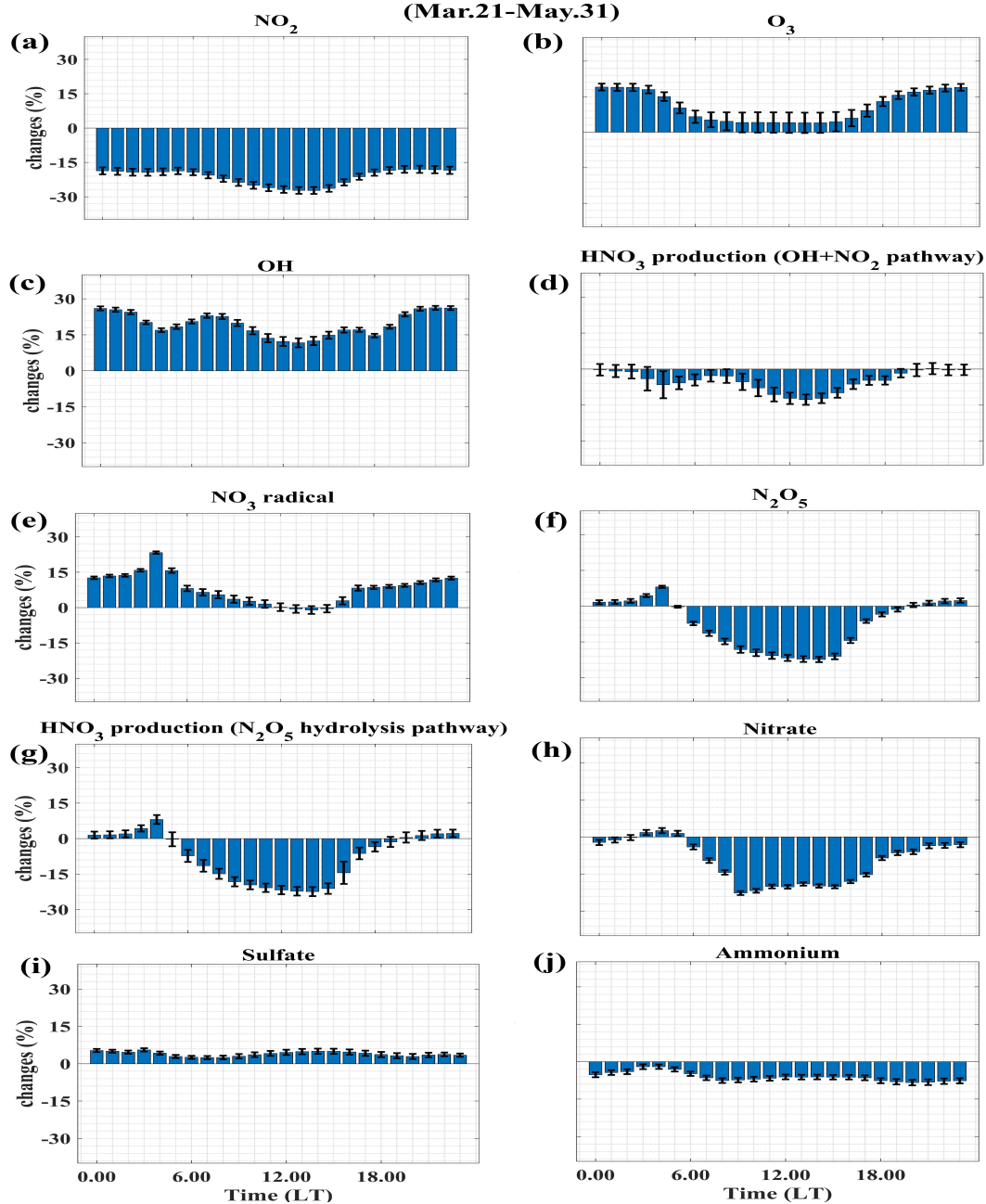
Figure 4. Diurnal cycle of emission accounted for GC NO_2, O_3, OH radical, HNO_3 production from oxidation of NO_2 by OH pathway, NO_3 radical, N_2O_5, HNO_3 production from N_2O_5 hydrolysis pathway, PM nitrate, sulfate, ammonium concentration changes between 2020 lockdown and 2020 BAU (no lockdown) scenario ($fX_{(GC,emi)}$). Error bars represent the standard error of respective hour in ten metropolitan areas.
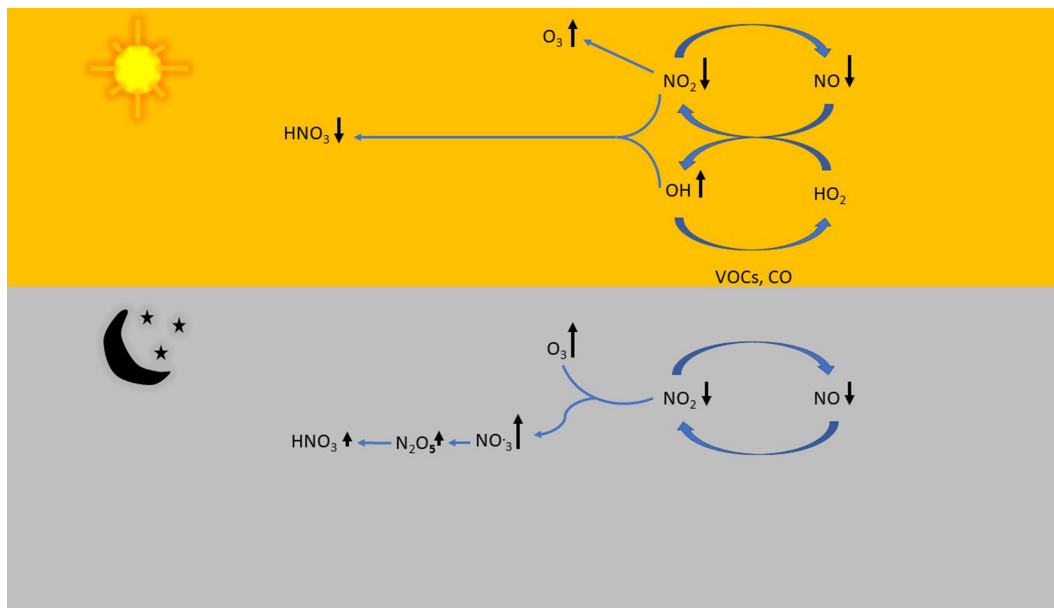
Figure 5. Generalized schematic diagram of day and night-time lockdown NO_X chemistry compared to BAU scenario.

~~HNO₃ production from N₂O₅ hydrolysis, resulting in slightly lower night-time lockdown PM nitrate compared to BAU (Fig. 4 (b,e,f,g))~~ However, higher night-time NO_3 levels result in relatively unchanged night-time HNO_3 production from N_2O_5 hydrolysis, resulting in slightly lower night-time lockdown PM nitrate compared to BAU (Fig. 4 (b,e,f,g)). This implies that the increase in NO_3 radical due to increased ozone partially offset the effect of reduced NO_X on nitrate formation. Previous studies have also shown that N_2O_5 hydrolysis plays important role in nitrate formation than the gas-phase day-time pathway (NO_2 + OH) (Allen et al., 2015; Chan et al., 2021; Kim et al., 2014; Liu et al., 2020; Yan et al., 2019). Figure 5 illustrates the conceptual model of generalized day and night-time lockdown NO_X chemistry compared to BAU scenario. The oxidation of SO_2 is a major source of sulfate, and the reaction with the OH radical dominates the gas-phase oxidation of SO_2 (Zhang et al., 2015). Therefore, the enhanced sulfate formation during the 2020 lockdown period could be due to the increased oxidizing capacity of atmosphere (OH) since we observe no significant change in emission accounted for GC SO_2 concentration, compared to BAU concentration (Fig. 3). Organic aerosol (OA) formation could be affected by the changes in oxidizing capacity of the atmosphere (Carlton et al., 2009), but no changes in emission accounted for GC lockdown OA were observed compared to 2020 BAU scenario. Therefore, the fact that no significant change in $PM_{2.5}$ due to lockdown restrictions is observed can be explained by a significant offset of the decreased day-time PM nitrate formation by enhanced formation of PM sulfate, while PM ammonium shows a marginal decrease.
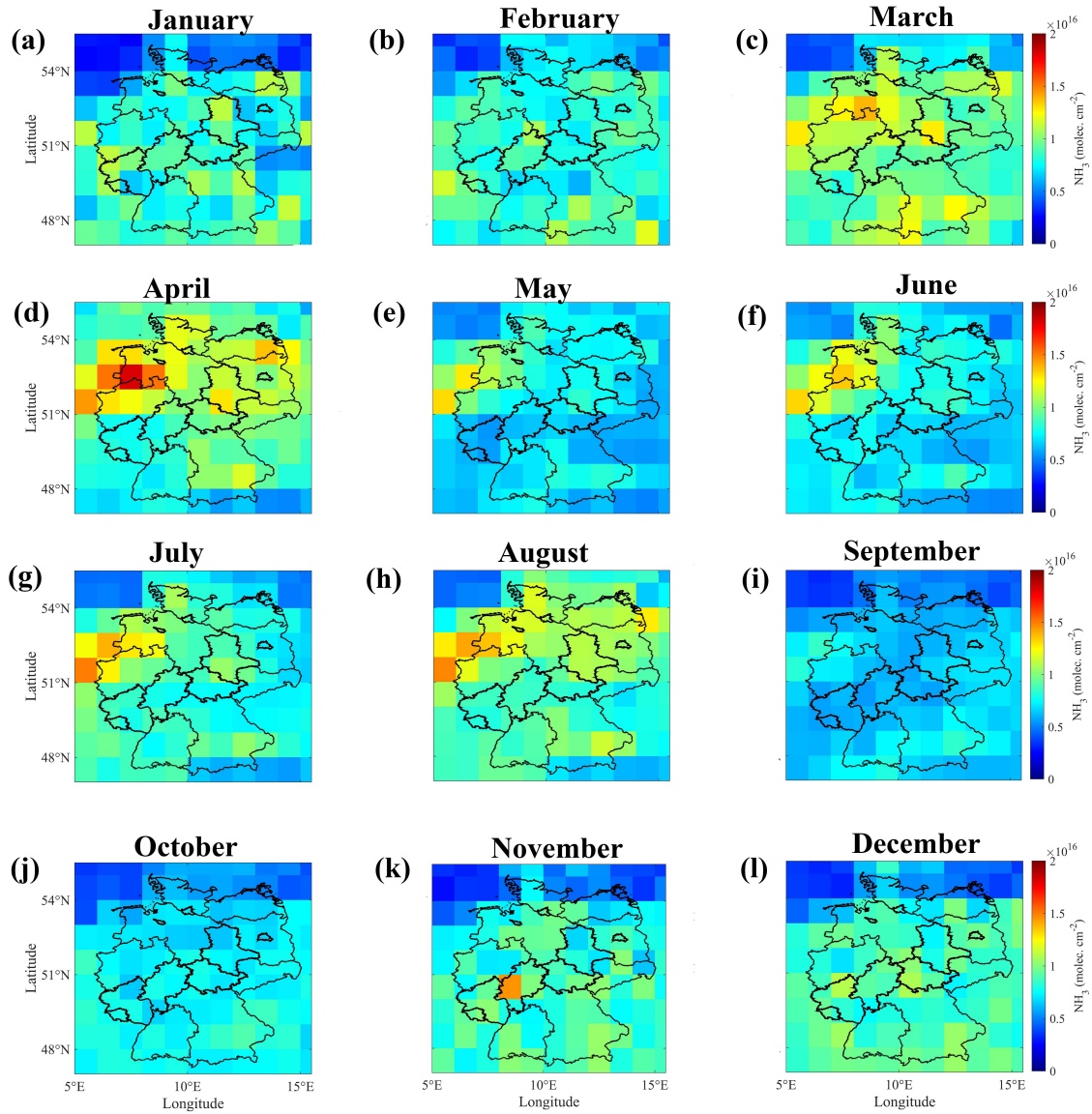
Figure 6. Monthly mean IASI NH₃ total column at 1*1 degree resolution.

4.3 Link between spring $PM_{2.5}$ pollution episodes and high NH_3 concentrations

It is worth noting that a significant fraction of $PM_{2.5}$ is PM nitrate. Ammonia (NH_3) is an important precursor for particulate
330 nitrate formation (Ansari and Pandis, 1998; Banzhaf et al., 2013; Behera and Sharma, 2010; Wu et al., 2016). This explains
the importance of monitoring and potentially regulating ammonia emissions. Therefore, the inter- and intra-annual changes in
ammonia (NH_3) concentrations over Germany, as well as their relationship to $PM_{2.5}$ variability, are reviewed and analyzed
further below. In Germany, atmospheric NH_3 levels follow a monthly pattern, with NH_3 levels peaking in April (Fig. 6). NH_3
levels are also elevated during summer months. In Europe, major agricultural practices (fertilizer and manure applications)
335 take place in the early spring (Petetin et al., 2016; Ramanantenasoa et al., 2018; Viatte et al., 2020). The higher atmospheric
ammonia levels in April are attributable to agricultural practices such as fertilizer application. The high NH_3 values in summer
are most likely due to warm climates (Kuttippurath et al., 2020). Monthly average NH_3 maps clearly show the high NH_3 values
over North-West Germany from April to August, with particularly high values in April. It indicates that North-West Germany
is a hotspot of ammonia emissions compared to the rest of the country. North-West Germany is known for its high livestock
340 density (livestock farming (EUR, 2013; Scarlat et al., 2018)) and it is dominated by crop and grass land (ESA, 2017). Livestock
farming and fertilizer application account for 75 % of NH_3 emissions in Europe (Webb et al., 2005). NH_3 concentrations in
Germany vary greatly from year to year (inter-annual variabilities). We consider the period between March 21 and April 30
when a stricter lockdown was in place to illustrate the inter-annual variability of atmospheric NH_3 between 2018 and 2020
(Fig. 7). NH_3 levels are lower in 2019 than in 2018, which can be attributed to the lower temperature in 2019 compared to
345 2018. Meanwhile, even though strict lockdown was in place, NH_3 levels in 2020 are higher than in 2019 and 2018, possibly
due to low precipitation. High temperatures promote NH_3 volatilization (increases the NH_3 level in the atmosphere) (Ernst
and Massey, 1960), whereas high rainfall favors wet deposition (removal of atmospheric NH_3). Schiferl et al. (2016); Viatte
et al. (2020) have also shown that meteorological parameters such as temperature and precipitation play a greater role in NH_3
inter-annual variability.

350   High PM pollution episodes are likely to occur frequently during the winter due to high residential heating demand and
favorable meteorological conditions (e.g., low temperature and inversion condition). However, high concentrations of $PM_{2.5}$
are apparent in German metropolitan areas in the early spring (from the second half of March to the end of April, e.g., Fig. 8 (a)
for ~~Cologne~~Munich metropolitan area). On March 21, 2020, the German government imposed COVID-19 lockdown restrictions.
However, in-situ $PM_{2.5}$ concentrations during the initial lockdown period are higher than during the pre-lockdown period in
355 2020. High $PM_{2.5}$ levels from the second half of March to the end of April are also consistent with previous years without
lockdown restrictions. ~~It is notable that this high spring $PM_{2.5}$ episodes are associated with high NH_3 concentrations (Fig. 6 (b)).~~ The high $PM_{2.5}$
events that occur in the spring have also been observed in other European cities, and they typically contain ammonium nitrate
and ammonium sulfate (Fortems-Cheiney et al., 2016; Renner and Wolke, 2010; Schaap et al., 2004; Viatte et al., 2020, 2021).
Above, we show the high NH_3 levels in early spring (April) and summer months. High $PM_{2.5}$ concentrations are evident in
360 spring, however, we did not observe high $PM_{2.5}$ episodes in summer (Fig. 8 (a)). It is also worth noting that even in the spring
and winter $PM_{2.5}$ is not consistently high on days with high NH_3. This reflects the complexity of the process of gas to particle

2018 (Mar.21-Apr.30)   **2019 (Mar.21-Apr.30)**   **2020 (Mar.21-Apr.30)**

IASI NH₃ total column

Temperature and Wind
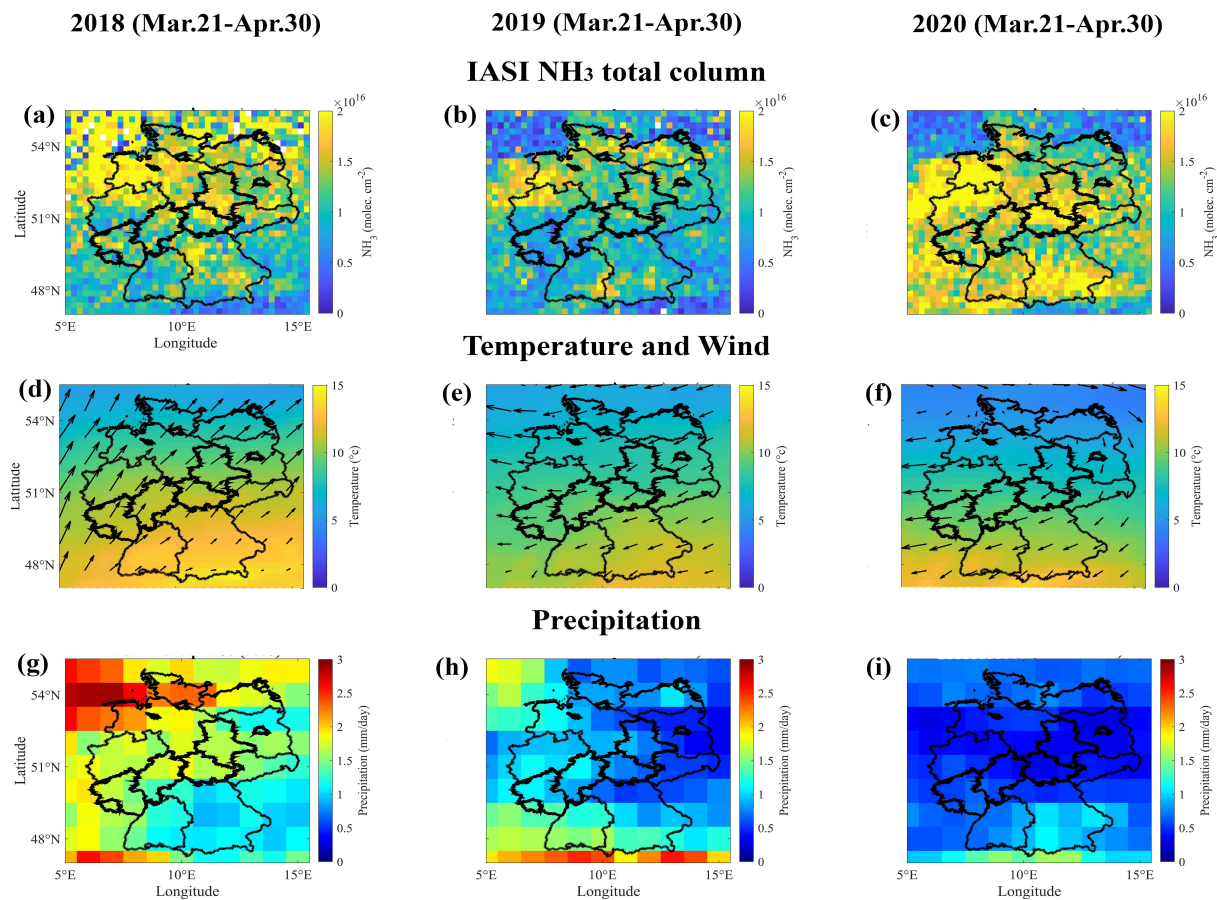
Precipitation

Figure 7. Mean IASI NH₃ total column (daily IASI NH₃ measurements gridded at 0.25 degree resolution) (top), mean temperature and wind (middle) and mean precipitation (bottom).

conversion. Despite high NH₃ concentrations, ammonia(NH₃)-to-ammonium(NH₄) conversion is mainly driven by various meteorological factors such as temperature (and relative humidity). Studies (Viatte et al., 2020; Wang et al., 2015; Watson et al., 1994) have shown that conditions such as temperature of less than 10 °C and a high relative humidity of more than 70

365 % are optimal for atmospheric gas-phase NH₃ to transform into ammonium salts, mainly due to reversible ammonium nitrate formation, which depends on temperature and relative humidity; warm and dry conditions partition ammonia back to the gas phase (Mozurkewich, 1993). In comparison to summer, the impact of NH₃ on PM₂.₅ formation is considerable for winter and spring over Europe (Viatte et al., 2020, 2021) and the US (Schiferl et al., 2016). Summer weather is typically warmer (and has lower relative humidity) than winter and spring, which could explain why high NH₃ concentrations are not associated with high

370 PM₂.₅ in summer or late spring. Furthermore, it is important to note that PM₂.₅ anthropogenic precursor emissions (NO$_X$, SO₂, VOCs) have a seasonal cycle, with higher emissions in winter than summer; however, biogenic VOC emissions dominate in the summer. ~~To further demonstrate this for German metropolitan areas~~To further demonstrate the relationship between PM₂.₅ and NH₃ for
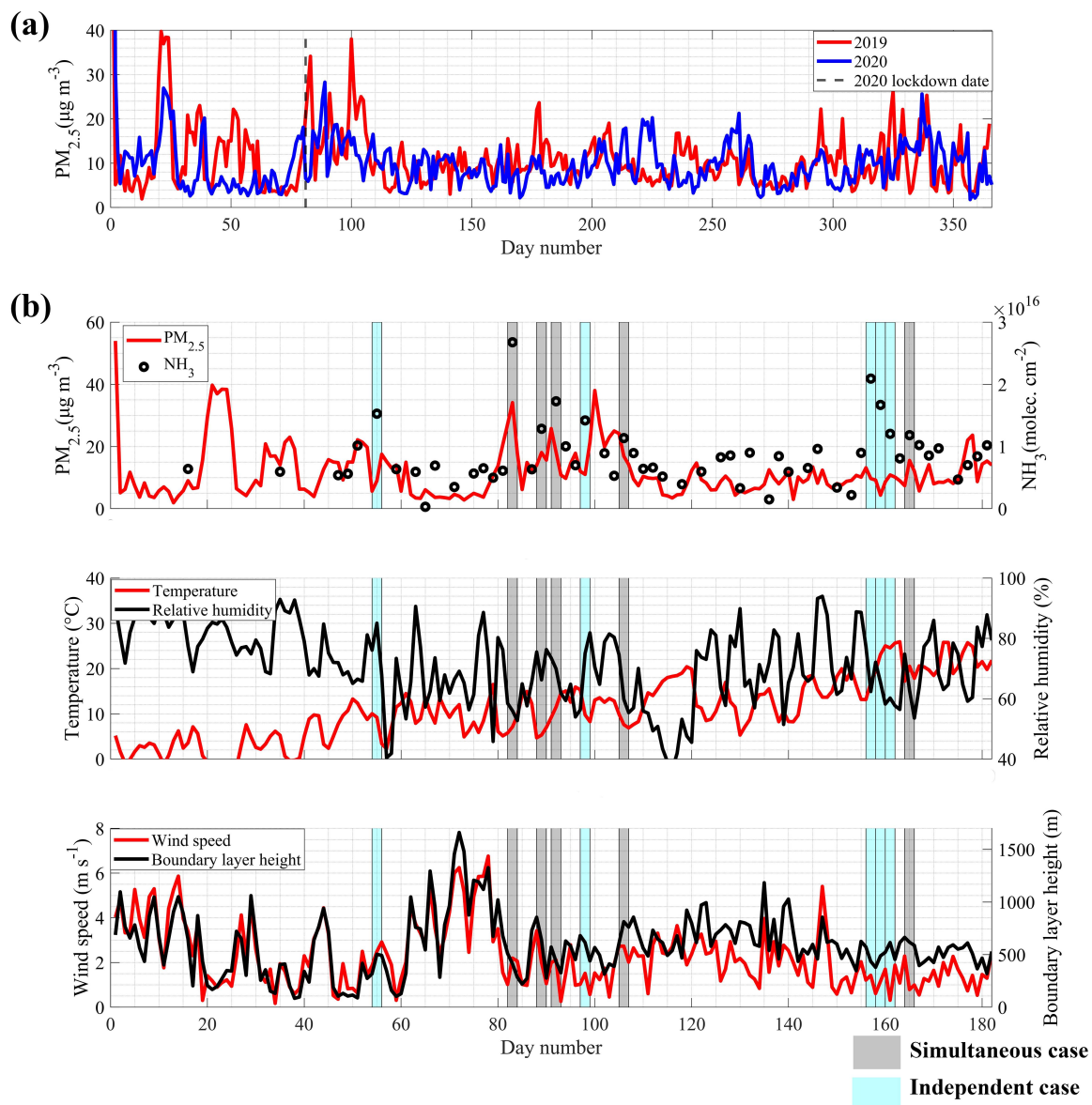
Figure 8. 2019 and 2020 annual daily mean in-situ $PM_{2.5}$ concentrations in Munich (a). In figure panel (a), the vertical dashed line denotes the start of 2020 lockdown. 2019 daily mean in-situ $PM_{2.5}$ and column NH_3 from IASI satellite (b, top). 2019 daily mean temperature and relative humidity (b, middle). 2019 daily mean wind speed and boundary layer height (b, bottom). The corresponding days for the cases "Simultaneous" are shaded with gray color and for the cases "Independent" are shaded with cyan color. "Simultaneous" - Simultaneous increase in NH_3 (IASI) and $PM_{2.5}$ (in-situ) concentrations on same day. "Independent" - Increase in NH_3 (IASI) concentration not corresponding to an increase in $PM_{2.5}$ (in-situ) concentration on same day.

German metropolitan areas, we consider two cases ("Simultaneous" and "Independent") for 2018 and 2019 (e.g., Fig. 8 (b) for

375 Munich metropolitan area). "Simultaneous" - Simultaneous increase in NH_3 (IASI) and $PM_{2.5}$ (in-situ) concentrations on same day. "Independent" - Increase in NH_3 (IASI) concentration not corresponding to an increase in $PM_{2.5}$ (in-situ) concentration on same day. As an example, for the ~~Cologne~~Munich metropolitan area, the temperature and boundary layer height for the "Simultaneous" case ~~(11.7±6.8 °C and 500.4±166.5 m, respectively)~~(14.8±8.3 °C and 557.9±193.4 m, respectively) is lower than for the "Independent" case ~~(13.4±6 °C and 628.9±274.3 m, respectively)~~(15.5±5.4 °C and 599.8±196.3 m, respectively). In addition to low temperature, low boundary layer height results in higher pollutant concentrations and can thus result in more intense

380 atmospheric chemical reactions. We found similar results for other metropolitan areas, but with different absolute values ~~(Fig. 6 (d))~~(Table C1). The regional differences are unsurprising, because other factors also influence the formation of $PM_{2.5}$ from NH_3 (e.g., other precursor concentrations such as NO_X and SO_X). However, these findings support previous studies and imply that low temperature and low boundary layer height are most favorable for the formation of $PM_{2.5}$ during the periods of high NH_3. ~~GC also simulates the high spring $PM_{2.5}$ concentrations that have been observed, with high ammonium (NH_4) concentrations (Fig. 6 (c)).~~

385 ## 5 Conclusions

Our study estimates the influence of anthropogenic emission reductions on $PM_{2.5}$ concentration changes during the 2020 lockdown period in German metropolitan areas. Mean meteorology accounted for $PM_{2.5}$ concentrations decreased by 5 % during the 2020 lockdown period (spring) compared to the corresponding period in 2019. However, during the 2020 pre-lockdown period (winter), meteorology accounted for $PM_{2.5}$ concentrations are 19 % lower than in 2019. Meanwhile, meteorology ac-

390 counted for NO_2 levels decreased 23 % during the 2020 lockdown period, which is a larger decrease than 2020 pre-lockdown period compared to 2019 (9 %). No significant change in meteorology accounted for SO_2 and CO concentrations were observed during the 2020 lockdown period, compared to 2019.

The GC model with the COVID-19 emission reduction scenario based on observations (23 % reduction in NO_X emission with unchanged VOC and SO_2) supports our findings of only a marginal decrease in $PM_{2.5}$ and a significant decrease in NO_2

395 levels. Due to being in a NO_X saturated ozone production regime, the GC lockdown OH and O_3 concentrations increased by 15 % and 9 %, respectively, compared to BAU levels. However, O_X analysis suggest that the only increase in ozone during the day-time is due to increased ozone production efficiency via NO_X saturated regime chemistry, whereas the increase at night-time is due to decreased NO titration. Despite an increase in OH radicals, the GC lockdown PM nitrate formation decreased significantly during the day, due to a significant decrease in NO_2, compared to the BAU scenario. Increased night-time ozone,

400 however, results in increased night-time NO_3, despite decreased NO_2, in turn, resulting in slightly increased night-time N_2O_5 concentration and only a small change in night-time PM nitrate. Overall this results in a small decrease in daily PM nitrate. In addition, the increased OH concentration results in a marginal increase of sulfate formation. Nitrate, sulfate, ammonium and organic aerosol are the major secondary components of $PM_{2.5}$. The decreased day-time PM nitrate is partially offset by the enhanced PM sulfate, and there is no significant impact from slightly decreased PM ammonium and no change in organic

405 aerosol, resulting in a marginal decrease in $PM_{2.5}$ concentrations during the lockdown period.

Based on our findings, we suggest that additional emission control measures aimed at reducing ozone pollution be implemented which should also help reduce PM. A concurrent reduction of NO_X and VOCs emissions should occur. Otherwise, ozone levels will rise as NO_X emissions drop, increasing oxidizing capacity, until a NO_X limited ozone production regime is reached. We also addressed the annual spring $PM_{2.5}$ pollution episodes in German metropolitan areas, which are associated with high NH_3 concentrations. North-West Germany is a hot-spot of NH_3 emissions, primarily emitted from livestock farming and intensive agricultural activities (fertilizer application), with high NH_3 concentrations in the early spring and summer months. Winter and spring meteorological conditions are more favorable for $PM_{2.5}$ formation from NH_3 than summer. Unsurprisingly, low temperature (and low boundary layer height) is shown to be a favorable meteorological condition for the formation of $PM_{2.5}$ from NH_3. Regulation of NH_3 emissions, primarily from agriculture, has the potential to reduce $PM_{2.5}$ pollution significantly in German metropolitan areas.

In this study, a COVID-19 emission reduction scenario was created using meteorology accounted for proxy pollutant concentration changes, assuming that observed proxy pollutant concentration changes are due to the combined direct effects of emission and meteorology changes. Our GC modeling study work reflects the assumed direct relationship between changes in meteorology accounted for NO_2 concentration and changes in NO_X emission. This work also shows a direct relationship between changes in meteorology accounted for SO_2 (and CO) concentration and changes in SO_X (and CO) emission. However, due to the non-linear feedback system in atmospheric chemistry, this assumption should be investigated further. Because of their similar sources, we use CO concentration as a proxy for anthropogenic VOC concentration. However, this is debatable because VOC is more reactive than CO. We call for further advancements in estimating the emission changes during the lockdown period, which would allow us to estimate the precise sensitivity of $PM_{2.5}$ to changes in emissions from various sources and comparison of VOC emission inventories with observations. This will help in the implementation of appropriate air quality regulation strategies in the future. Organic aerosol accounts for nearly 30 % of total $PM_{2.5}$, which could be influenced by both primary/secondary biogenic and anthropogenic sources. However, our study is limited to examining the effects of NO_X emission changes on $PM_{2.5}$ formation. Therefore, future studies on VOC emission changes on OA formation during high PM pollution episodes, particularly in the spring, will be more important in mitigating PM pollution.

Data availability. Hourly measurements of in-situ NO_2, O_3, $PM_{2.5}$, SO_2 and CO data are downloaded from (https://discomap.eea.europa.eu/map/fme/AirQualityExport.htm). The TROPOMI SO_2 data are obtained from https://s5phub.copernicus.eu/. The IASI NH_3 data are obtained from https://iasi.aeris-data.fr/catalog/. Hourly ERA5 meteorological data are available at https://cds.climate.copernicus.eu/.

Table A1. The statistical evaluation (R, RMSE and mean bias) of the GC model performance (PM$_{2.5}$) for the 2019 study period (January 1 to May 31).

Metropolitan area	Correlation coefficient (R)	RMSE (μg m^{-3})	Mean bias (GC – insitu / insitu) (%)
Bremen	0.6	8.7	-18.9
Cologne	0.5	11	11.7
Dresden	0.56	9.2	-18.8
Dusseldorf	0.53	10.5	-15.7
Frankfurt	0.58	9.3	-37.4
Hamburg	0.67	8	-12.7
Hanover	0.59	7.9	-13.1
Leipzig	0.39	8.4	-28.6
Munich	0.5	8.5	-18.6
Stuttgart	0.53	8.6	-16.1

Table B1. The statistical evaluation (R, RMSE and mean bias) of the GC model performance (nitrate and ammonium in PM$_{2.5}$) for the 2019 study period (January 1 to May 31). For this comparison, data from the urban measurement station (14.33°E, 51.75°N) in Germany is used.

Species	Correlation coefficient (R)	RMSE (μg m^{-3})	Mean bias (GC – insitu / insitu) (%)
Nitrate	0.51	2.33	-32.1
Ammonium	0.45	1.34	37

Table C1. The Statistical distribution of meteorological parameters for the cases "Independent" (each row top) and "Simultaneous" (each row bottom) in ten German metropolitan areas for 2018 and 2019.

Metropolitan area	Number of days	Wind speed (m/s)	Temperature (° C)	RH (%)	PBL height (m)
Bremen	17	4.3 ± 2.1	13.6 ± 5.8	62.3 ±14.1	625.5 ± 211.1
	27	4.5 ± 2	11.5 ± 7	67.3 ± 16	541 ± 212.5
Cologne	16	3±2.2	13.4±6.1	74.3±11.4	628.9±274.31
	24	3.2±1.7	11.7±6.8	65.3±14.4	500.4±166.4
Dresden	24	1.9±1.1	14.9±6.9	68.6±12.8	578.9±220.7
	20	2.4±0.8	11.1±7.4	66.3±11	592.1±208.8
Dusseldorf	10	3.4±2.1	13.2±4.8	69±11.3	732.1±311.8
	30	3.4±1.8	13.5±5.6	66.2±13.5	494±168
Frankfurt	18	3.2±1.8	13.1±6.3	64.9±13.2	695.2±284.1
	21	2.2±1.1	13.1±6.6	63.6±13.6	442.8±194.5
Hamburg	14	5.4±2.5	13.7±6.5	57.5±11.8	705.3±249.2
	27	5.2±2.3	11.1±3.3	67.7±15	674.1±262
Hannover	14	3.2±2	14.2±7.8	62.5±10.4	697.5±210.2
	24	3.8±1.9	9.3±7.6	67.6±13.1	557.5±176.3
Leipzig	18	2.9±1.4	14.9±8	63.7±12.7	674.6±206.3
	30	3.4±1.6	11.2±7.1	61.9±10.8	532.3±227.3
Munich	26	2±1.1	15.5±5.4	71.5±12.3	599.8±196.3
	17	1.6±0.8	14.8±8.3	65.4±9.8	557.9±193.4
Stuttgart	22	1.9±0.9	13.8±6.4	71.7±11	600.7±234.9
	22	1.5±0.6	13.7±6.3	67.3±12.9	449±191.1
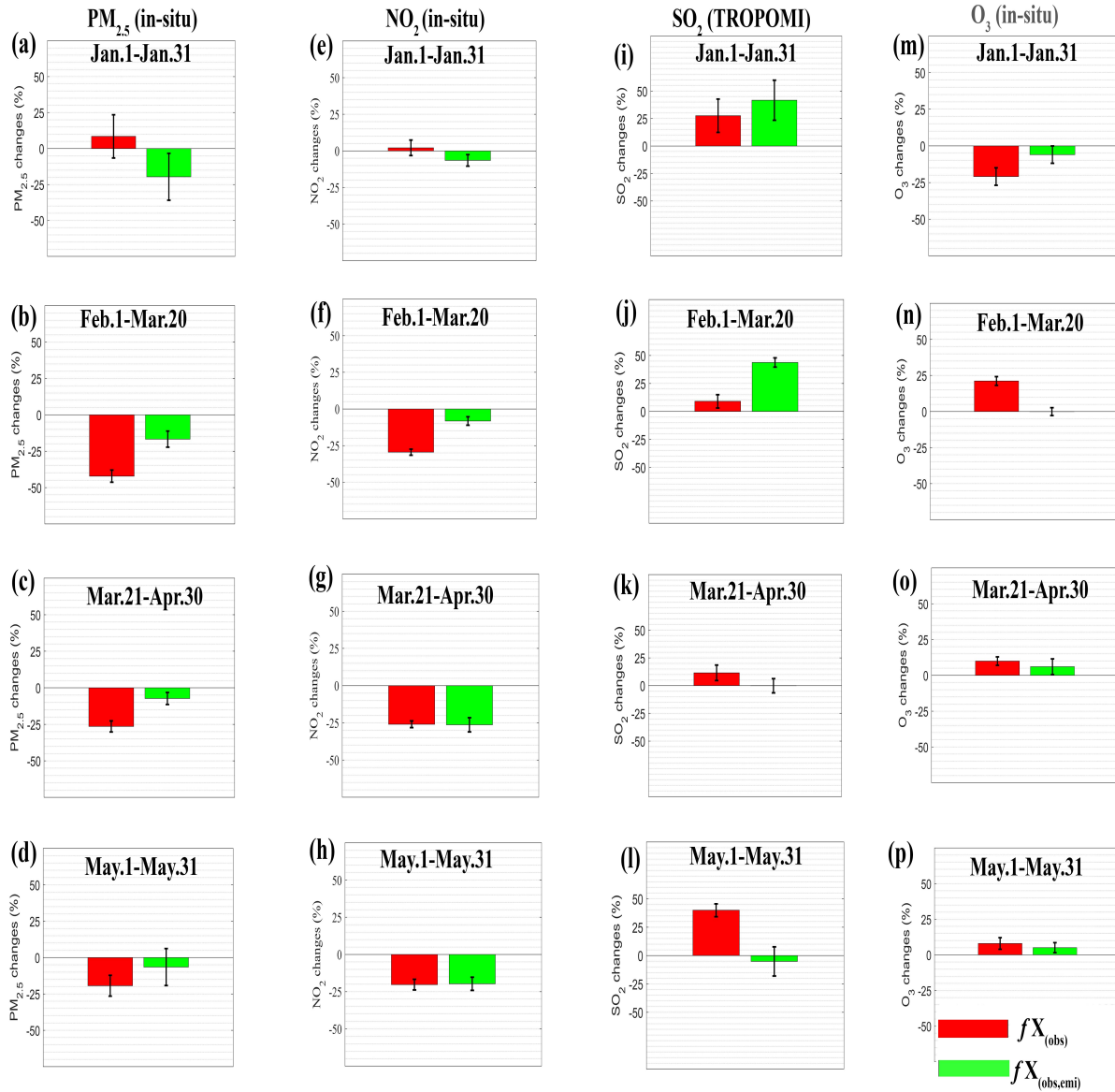
Figure A1. Meteorology unaccounted for (red) and meteorology accounted for (green) mean changes in $PM_{2.5}$, NO_2, SO_2 and O_3 concentrations between 2020 and 2019 in ten German metropolitan areas. Error bars represent the 1 σ of mean of ten metropolitan areas.
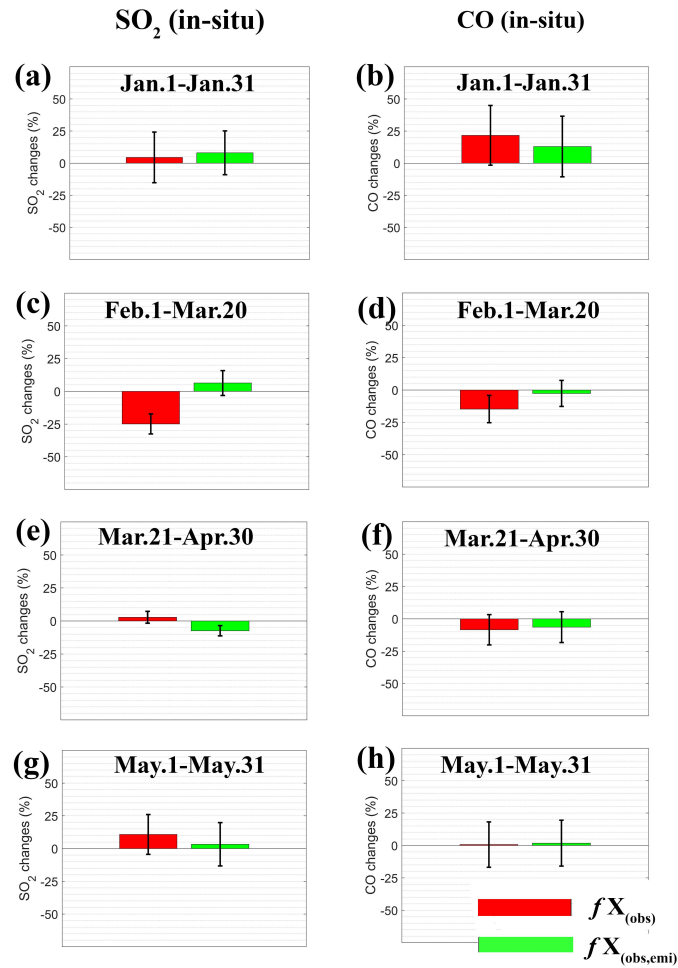
Figure B1. Meteorology unaccounted for (red) and meteorology accounted for (green) mean changes in in-situ SO_2 (Bremen, Dresden, Frankfurt, Hamburg and Leipzig) and in in-situ CO (Bremen, Frankfurt, Hamburg, Hanover, Munich and Stuttgart) between 2020 and 2019. Error bars represent the 1σ of mean of above mentioned metropolitan areas.
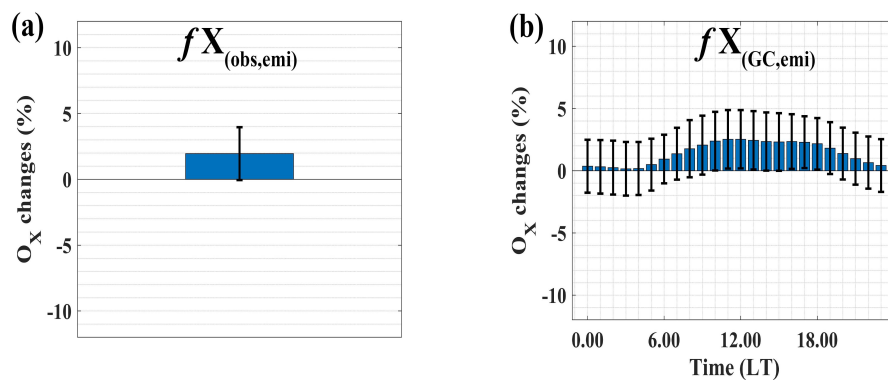
Figure C1. Meteorology accounted for mean changes in in-situ O_X between 2020 and 2019 (left). Diurnal cycle of emission accounted for GC O_X concentration changes between 2020 lockdown and 2020 BAU (no lockdown) scenario (right). Error bars represent the 1 σ of mean of ten metropolitan areas.

2019
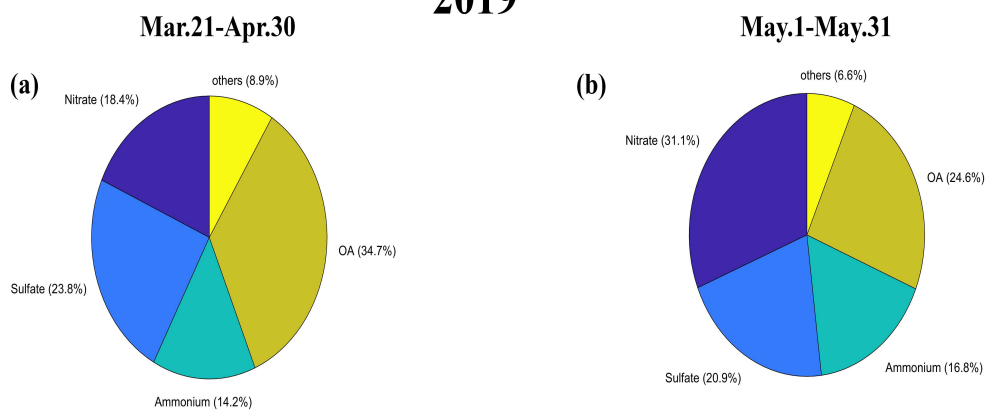
Figure D1. Mean relative contributions of PM$_{2.5}$ species simulated by GC for 2019.

2020 (BAU)

Mar.21-Apr.30   **May.1-May.31**
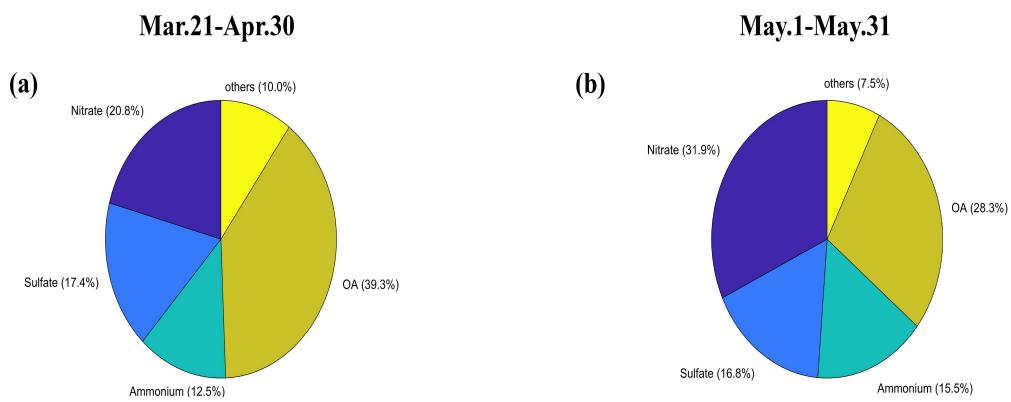
Figure E1. Mean relative contributions of PM$_{2.5}$ species simulated by GC for 2020 (no lockdown).

2020 (lockdown)
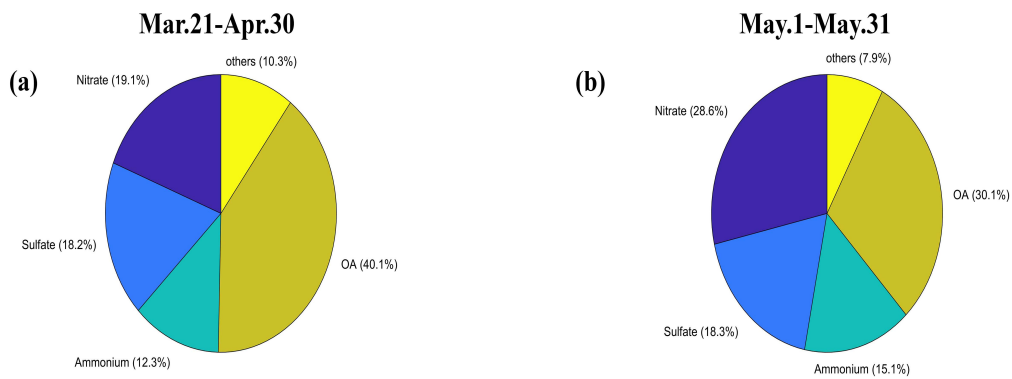
Figure F1. Mean relative contributions of PM$_{2.5}$ species simulated by GC for 2020 (lockdown).

Author contributions. VB, and XB obtained the measurement data; ZQ performed the modeling work; VB analyzed the data and wrote the manuscript draft; JC, and FK supervised the work and edited the manuscript.

435 *Competing interests.* The authors declare that they have no conflict of interest.

Acknowledgements. Vigneshkumar Balamurugan, Jia Chen, and Xiao Bi are supported by Institute for Advanced Study, Technical University of Munich, through the German Excellence Initiative and the European Union Seventh Framework Program (Grant: 291763) and in part by the German Research Foundation (DFG) (Grant: 419317138). Frank N. Keutsch is funded and supported by the Harvard' Solar Geoengineering Research Program.

440 References

EUROSAT, Livestock density by NUTS 2 regions, EU-28, 2013. https://ec.europa.eu/eurostat/statistics-explained/index.php?title=File:Livestock_density_by_NUTS_2_regions,_EU-28,_2013.png, 2013.

ESA, Mapping Germany's agricultural landscape. https://www.esa.int/ESA_Multimedia/Images/2017/08/Mapping_Germany_s_agricultural_landscape, 2017.

445 SO2 emission (EEA), Indicator Assessment:Sulphur dioxide (SO2) emissions. https://www.eea.europa.eu/data-and-maps/indicators/eea-32-sulphur-dioxide-so2-emissions-1/assessment-3, 2021.

Allen, H. M., Draper, D. C., Ayres, B. R., Ault, A., Bondy, A., Takahama, S., Modini, R. L., Baumann, K., Edgerton, E., Knote, C., et al.: Influence of crustal dust and sea spray supermicron particle concentrations and acidity on inorganic NO 3- aerosol during the 2013 Southern Oxidant and Aerosol Study, Atmospheric Chemistry and Physics, 15, 10 669–10 685, 2015.

450 Ansari, A. S. and Pandis, S. N.: Response of inorganic PM to precursor concentrations, Environmental Science & Technology, 32, 2706–2714, 1998.

Ayres, B., Allen, H., Draper, D., Brown, S., Wild, R., Jimenez, J., Day, D., Campuzano-Jost, P., Hu, W. d., Gouw, J. d., et al.: Organic nitrate aerosol formation via NO 3+ biogenic volatile organic compounds in the southeastern United States, Atmospheric Chemistry and Physics, 15, 13 377–13 392, 2015.

455 Baker, A. K., Beyersdorf, A. J., Doezema, L. A., Katzenstein, A., Meinardi, S., Simpson, I. J., Blake, D. R., and Rowland, F. S.: Measurements of nonmethane hydrocarbons in 28 United States cities, Atmospheric Environment, 42, 170–182, 2008.

Balamurugan, V., Chen, J., Qu, Z., Bi, X., Gensheimer, J., Shekhar, A., Bhattacharjee, S., and Keutsch, F. N.: Tropospheric NO2 and O3 response to COVID-19 lockdown restrictions at the national and urban scales in Germany, Journal of Geophysical Research: Atmospheres, 126, 2021.

460 Banzhaf, S., Schaap, M., Wichink Kruit, R. J., Denier Van Der Gon, H., Stern, R., and Builtjes, P.: Impact of emission changes on secondary inorganic aerosol episodes across Germany, Atmospheric Chemistry and Physics, 13, 11 675–11 693, 2013.

Barré, J., Petetin, H., Colette, A., Guevara, M., Peuch, V.-H., Rouil, L., Engelen, R., Inness, A., Flemming, J., Pérez García-Pando, C., et al.: Estimating lockdown induced European NO 2 changes, Atmospheric Chemistry and Physics Discussions, pp. 1–28, 2020.

Bauer, S., Koch, D., Unger, N., Metzger, S., Shindell, D., and Streets, D.: Nitrate aerosols today and in 2030: a global simulation including 465 aerosols and tropospheric ozone, Atmospheric Chemistry and Physics, 7, 5043–5059, 2007.

Bauwens, M., Compernolle, S., Stavrakou, T., Müller, J.-F., Van Gent, J., Eskes, H., Levelt, P. F., van der A, R., Veefkind, J., Vlietinck, J., et al.: Impact of coronavirus outbreak on NO2 pollution assessed using TROPOMI and OMI observations, Geophysical Research Letters, 47, e2020GL087 978, 2020.

Behera, S. N. and Sharma, M.: Investigating the potential role of ammonia in ion chemistry of fine particulate matter formation for an urban 470 environment, Science of the Total Environment, 408, 3569–3575, 2010.

Biswal, A., Singh, T., Singh, V., Ravindra, K., and Mor, S.: COVID-19 lockdown and its impact on tropospheric NO2 concentrations over India using satellite-based data, Heliyon, 6, e04 764, 2020.

Blanchard, C. L. and Tanenbaum, S. J.: Differences between weekday and weekend air pollutant levels in southern California, Journal of the Air & Waste Management Association, 53, 816–828, 2003.

475 Campbell, P. C., Tong, D., Tang, Y., Baker, B., Lee, P., Saylor, R., Stein, A., Ma, S., Lamsal, L., and Qu, Z.: Impacts of the COVID-19 Economic Slowdown on Ozone Pollution in the US, Atmospheric Environment, p. 118713, 2021.

Carlton, A., Wiedinmyer, C., and Kroll, J.: A review of Secondary Organic Aerosol (SOA) formation from isoprene, Atmospheric Chemistry and Physics, 9, 4987–5005, 2009.

Cesari, D., De Benedetto, G., Bonasoni, P., Busetto, M., Dinoi, A., Merico, E., Chirizzi, D., Cristofanelli, P., Donateo, A., Grasso, F., et al.: Seasonal variability of PM2. 5 and PM10 composition and sources in an urban background site in Southern Italy, Science of the Total Environment, 612, 202–213, 2018.

Chan, Y.-C., Evans, M. J., He, P., Holmes, C. D., Jaeglé, L., Kasibhatla, P., Liu, X.-Y., Sherwen, T., Thornton, J. A., Wang, X., et al.: Heterogeneous nitrate production mechanisms in intense haze events in the North China Plain, Journal of Geophysical Research: Atmospheres, 126, e2021JD034 688, 2021.

Chang, W. L., Bhave, P. V., Brown, S. S., Riemer, N., Stutz, J., and Dabdub, D.: Heterogeneous atmospheric chemistry, ambient measurements, and model calculations of N2O5: A review, Aerosol Science and Technology, 45, 665–695, 2011.

Chang, W. L., Brown, S. S., Stutz, J., Middlebrook, A. M., Bahreini, R., Wagner, N. L., Dubé, W. P., Pollack, I. B., Ryerson, T. B., and Riemer, N.: Evaluating N2O5 heterogeneous hydrolysis parameterizations for CalNex 2010, Journal of Geophysical Research: Atmospheres, 121, 5051–5070, 2016.

Clark, H., Bennouna, Y., Tsivlidou, M., Wolff, P., Sauvage, B., Barret, B., Le Flochmoën, E., Blot, R., Boulanger, D., Cousin, J.-M., et al.: The Effects of the COVID-19 Lockdowns on the Composition of the Troposphere as Seen by IAGOS, Atmospheric Chemistry and Physics Discussions, pp. 1–33, 2021.

Clerbaux, C., Boynard, A., Clarisse, L., George, M., Hadji-Lazaro, J., Herbin, H., Hurtmans, D., Pommier, M., Razavi, A., Turquety, S., et al.: Monitoring of atmospheric composition using the thermal infrared IASI/MetOp sounder, Atmospheric Chemistry and Physics, 9, 6041–6054, 2009.

Collivignarelli, M. C., Abbà, A., Bertanza, G., Pedrazzani, R., Ricciardi, P., and Miino, M. C.: Lockdown for CoViD-2019 in Milan: What are the effects on air quality?, Science of the total environment, 732, 139 280, 2020.

Deroubaix, A., Brasseur, G., Gaubert, B., Labuhn, I., Menut, L., Siour, G., and Tuccella, P.: Response of surface ozone concentration to emission reduction and meteorology during the COVID-19 lockdown in Europe, Meteorological Applications, 28, e1990, 2021.

Dietrich, F., Chen, J., Voggenreiter, B., Aigner, P., Nachtigall, N., and Reger, B.: MUCCnet: Munich Urban Carbon Column network, Atmospheric Measurement Techniques, 14, 1111–1126, 2021.

Doumbia, T., Granier, C., Elguindi, N., Bouarar, I., Darras, S., Brasseur, G., Gaubert, B., Liu, Y., Shi, X., Stavrakou, T., et al.: Changes in global air pollutant emissions during the COVID-19 pandemic: a dataset for atmospheric chemistry modeling, Earth System Science Data Discussions, pp. 1–26, 2021.

Erisman, J. and Schaap, M.: The need for ammonia abatement with respect to secondary PM reductions in Europe, Environmental Pollution, 129, 159–163, 2004.

Ernst, J. and Massey, H.: The effects of several factors on volatilization of ammonia formed from urea in the soil, Soil Science Society of America Journal, 24, 87–90, 1960.

Field, R. D., Hickman, J. E., Geogdzhayev, I. V., Tsigaridis, K., and Bauer, S. E.: Changes in satellite retrievals of atmospheric composition over eastern China during the 2020 COVID-19 lockdowns, Atmospheric Chemistry and Physics Discussions, pp. 1–31, 2020.

Filonchyk, M., Hurynovich, V., and Yan, H.: Impact of Covid-19 lockdown on air quality in the Poland, Eastern Europe, Environmental Research, 198, 110 454, 2021.

Fisher, J. A., Jacob, D. J., Travis, K. R., Kim, P. S., Marais, E. A., Chan Miller, C., Yu, K., Zhu, L., Yantosca, R. M., Sulprizio, M. P., et al.: Organic nitrate chemistry and its implications for nitrogen budgets in an isoprene- and monoterpene-rich atmosphere: constraints from

515   aircraft (SEAC 4 RS) and ground-based (SOAS) observations in the Southeast US, Atmospheric chemistry and physics, 16, 5969–5991, 2016.

Fortems-Cheiney, A., Dufour, G., Hamaoui-Laguel, L., Foret, G., Siour, G., Van Damme, M., Meleux, F., Coheur, P.-F., Clerbaux, C., Clarisse, L., et al.: Unaccounted variability in NH3 agricultural sources detected by IASI contributing to European spring haze episode, Geophysical Research Letters, 43, 5475–5482, 2016.

520   Fujita, E. M., Campbell, D. E., Zielinska, B., Sagebiel, J. C., Bowen, J. L., Goliff, W. S., Stockwell, W. R., and Lawson, D. R.: Diurnal and weekday variations in the source contributions of ozone precursors in California's South Coast Air Basin, Journal of the Air & Waste Management Association, 53, 844–863, 2003.

Fuzzi, S., Baltensperger, U., Carslaw, K., Decesari, S., Denier van der Gon, H., Facchini, M. C., Fowler, D., Koren, I., Langford, B., Lohmann, U., et al.: Particulate matter, air quality and climate: lessons learned and future needs, Atmospheric chemistry and physics, 15, 8217–8299, 525   2015.

Gaubert, B., Bouarar, I., Doumbia, T., Liu, Y., Stavrakou, T., Deroubaix, A., Darras, S., Elguindi, N., Granier, C., Lacey, F., et al.: Global changes in secondary atmospheric pollutants during the 2020 COVID-19 pandemic, Journal of Geophysical Research: Atmospheres, 126, e2020JD034 213, 2021.

Gensheimer, J., Turner, A. J., Shekhar, A., Wenzel, A., Keutsch, F. N., and Chen, J.: What are different measures of mobility telling 530   us about surface transportation CO2 emissions during the COVID-19 pandemic?, Journal of Geophysical Research: Atmospheres, p. e2021JD034664, 2021.

Geyer, A., Alicke, B., Konrad, S., Schmitz, T., Stutz, J., and Platt, U.: Chemistry and oxidation capacity of the nitrate radical in the continental boundary layer near Berlin, Journal of Geophysical Research: Atmospheres, 106, 8013–8025, 2001.

Goldberg, D. L., Anenberg, S. C., Griffin, D., McLinden, C. A., Lu, Z., and Streets, D. G.: Disentangling the impact of the COVID-19 535   lockdowns on urban NO2 from natural variability, Geophysical Research Letters, 47, e2020GL089 269, 2020.

Grange, S. K., Lee, J. D., Drysdale, W. S., Lewis, A. C., Hueglin, C., Emmenegger, L., and Carslaw, D. C.: COVID-19 lockdowns highlight a risk of increasing ozone pollution in European urban areas, Atmospheric Chemistry and Physics Discussions, pp. 1–25, 2020.

Guevara, M., Jorba, O., Soret, A., Petetin, H., Bowdalo, D., Serradell, K., Tena, C., Denier van der Gon, H., Kuenen, J., Peuch, V.-H., et al.: Time-resolved emission reductions for atmospheric chemistry modelling in Europe during the COVID-19 lockdowns, Atmospheric 540   Chemistry and Physics, 21, 773–797, 2021.

Hallquist, M., Wenger, J. C., Baltensperger, U., Rudich, Y., Simpson, D., Claeys, M., Dommen, J., Donahue, N., George, C., Goldstein, A., et al.: The formation, properties and impact of secondary organic aerosol: current and emerging issues, Atmospheric chemistry and physics, 9, 5155–5236, 2009.

Hammer, M. S., van Donkelaar, A., Martin, R. V., McDuffie, E. E., Lyapustin, A., Sayer, A. M., Hsu, N. C., Levy, R. C., Garay, M. J., 545   Kalashnikova, O. V., et al.: Effects of COVID-19 lockdowns on fine particulate matter concentrations, Science Advances, 7, eabg7670, 2021.

He, C., Hong, S., Zhang, L., Mu, H., Xin, A., Zhou, Y., Liu, J., Liu, N., Su, Y., Tian, Y., et al.: Global, continental, and national variation in PM2. 5, O3, and NO2 concentrations during the early 2020 COVID-19 lockdown, Atmospheric pollution research, 12, 136–145, 2021.

Hersbach, H., Bell, B., Berrisford, P., Hirahara, S., Horányi, A., Muñoz-Sabater, J., Nicolas, J., Peubey, C., Radu, R., Schepers, D., et al.: 550   The ERA5 global reanalysis, Quarterly Journal of the Royal Meteorological Society, 146, 1999–2049, 2020.

Higham, J., Ramírez, C. A., Green, M., and Morse, A.: UK COVID-19 lockdown: 100 days of air pollution reduction?, Air Quality, Atmosphere & Health, 14, 325–332, 2021.

Hoesly, R. M., Smith, S. J., Feng, L., Klimont, Z., Janssens-Maenhout, G., Pitkanen, T., Seibert, J. J., Vu, L., Andres, R. J., Bolt, R. M., et al.: Historical (1750–2014) anthropogenic emissions of reactive gases and aerosols from the Community Emissions Data System (CEDS), Geoscientific Model Development, 11, 369–408, 2018.

Hörmann, S., Jammoul, F., Kuenzer, T., and Stadlober, E.: Separating the impact of gradual lockdown measures on air pollutants from seasonal variability, Atmospheric pollution research, 12, 84–92, 2021.

Huang, X., Ding, A., Gao, J., Zheng, B., Zhou, D., Qi, X., Tang, R., Wang, J., Ren, C., Nie, W., et al.: Enhanced secondary pollution offset reduction of primary emissions during COVID-19 lockdown in China, National Science Review, 8, nwaa137, 2021.

Hudman, R., Moore, N., Martin, R., Russell, A., Mebust, A., Valin, L., and Cohen, R.: A mechanistic model of global soil nitric oxide emissions: implementation and space based-constraints., Atmospheric Chemistry & Physics Discussions, 12, 2012.

Jacob, D. J.: Introduction to atmospheric chemistry, Princeton University Press, 1999.

Jacobson, M. Z.: Fundamentals of atmospheric modeling, Cambridge university press, 1999.

Jiménez, P., Parra, R., Gasso, S., and Baldasano, J. M.: Modeling the ozone weekend effect in very complex terrains: a case study in the Northeastern Iberian Peninsula, Atmospheric environment, 39, 429–444, 2005.

Juda-Rezler, K., Reizer, M., Maciejewska, K., Błaszczak, B., and Klejnowski, K.: Characterization of atmospheric PM2. 5 sources at a Central European urban background site, Science of the Total Environment, 713, 136 729, 2020.

Kang, M., Zhang, J., Zhang, H., and Ying, Q.: On the Relevancy of Observed Ozone Increase during COVID-19 Lockdown to Summertime Ozone and PM2. 5 Control Policies in China, Environmental Science & Technology Letters, 8, 289–294, 2021.

Kang, Y.-H., You, S., Bae, M., Kim, E., Son, K., Bae, C., Kim, Y., Kim, B.-U., Kim, H. C., and Kim, S.: The impacts of COVID-19, meteorology, and emission control policies on PM 2.5 drops in Northeast Asia, Scientific reports, 10, 1–8, 2020.

Keller, C. A., Evans, M. J., Knowland, K. E., Hasenkopf, C. A., Modekurty, S., Lucchesi, R. A., Oda, T., Franca, B. B., Mandarino, F. C., Díaz Suárez, M. V., et al.: Global impact of COVID-19 restrictions on the surface concentrations of nitrogen dioxide and ozone, Atmospheric Chemistry and Physics, 21, 3555–3592, 2021.

Kim, Y. J., Spak, S. N., Carmichael, G. R., Riemer, N., and Stanier, C. O.: Modeled aerosol nitrate formation pathways during wintertime in the Great Lakes region of North America, Journal of Geophysical Research: Atmospheres, 119, 12–420, 2014.

Koukouli, M.-E., Skoulidou, I., Karavias, A., Parcharidis, I., Balis, D., Manders, A., Segers, A., Eskes, H., and van Geffen, J.: Sudden changes in nitrogen dioxide emissions over Greece due to lockdown after the outbreak of COVID-19, Atmospheric Chemistry and Physics, 21, 1759–1774, 2021.

Kroll, J. H., Heald, C. L., Cappa, C. D., Farmer, D. K., Fry, J. L., Murphy, J. G., and Steiner, A. L.: The complex chemical effects of COVID-19 shutdowns on air quality, Nature Chemistry, 12, 777–779, 2020.

Kuttippurath, J., Singh, A., Dash, S., Mallick, N., Clerbaux, C., Van Damme, M., Clarisse, L., Coheur, P.-F., Raj, S., Abbhishek, K., et al.: Record high levels of atmospheric ammonia over India: Spatial and temporal analyses, Science of the Total Environment, 740, 139 986, 2020.

Le Quéré, C., Jackson, R. B., Jones, M. W., Smith, A. J., Abernethy, S., Andrew, R. M., De-Gol, A. J., Willis, D. R., Shan, Y., Canadell, J. G., et al.: Temporary reduction in daily global CO 2 emissions during the COVID-19 forced confinement, Nature Climate Change, pp. 1–7, 2020.

Lee, J. D., Drysdale, W. S., Finch, D. P., Wilde, S. E., and Palmer, P. I.: UK surface NO 2 levels dropped by 42% during the COVID-19 lockdown: impact on surface O 3, Atmospheric Chemistry and Physics, 20, 15 743–15 759, 2020.

590 Liu, L., Bei, N., Hu, B., Wu, J., Liu, S., Li, X., Wang, R., Liu, Z., Shen, Z., and Li, G.: Wintertime nitrate formation pathways in the north China plain: Importance of N2O5 heterogeneous hydrolysis, Environmental Pollution, 266, 115 287, 2020.

Marais, E. A., Jacob, D. J., Jimenez, J. L., Campuzano-Jost, P., Day, D. A., Hu, W., Krechmer, J., Zhu, L., Kim, P. S., Miller, C. C., et al.: Aqueous-phase mechanism for secondary organic aerosol formation from isoprene: application to the southeast United States and co-benefit of SO 2 emission controls, Atmospheric Chemistry and Physics, 16, 1603–1618, 2016.

595 Matthias, V., Quante, M., Arndt, J. A., Badeke, R., Fink, L., Petrik, R., Feldner, J., Schwarzkopf, D., Link, E.-M., Ramacher, M. O., et al.: The role of emission reductions and the meteorological situation for air quality improvements during the COVID-19 lockdown period in Central Europe, Atmospheric Chemistry and Physics, 21, 13 931–13 971, 2021.

Mendez-Espinosa, J. F., Rojas, N. Y., Vargas, J., Pachón, J. E., Belalcazar, L. C., and Ramírez, O.: Air quality variations in Northern South America during the COVID-19 lockdown, Science of the Total Environment, 749, 141 621, 2020.

600 Menut, L., Bessagnet, B., Siour, G., Mailler, S., Pennel, R., and Cholakian, A.: Impact of lockdown measures to combat Covid-19 on air quality over western Europe, Science of the Total Environment, 741, 140 426, 2020.

Mollner, A. K., Valluvadasan, S., Feng, L., Sprague, M. K., Okumura, M., Milligan, D. B., Bloss, W. J., Sander, S. P., Martien, P. T., Harley, R. A., et al.: Rate of gas phase association of hydroxyl radical and nitrogen dioxide, Science, 330, 646–649, 2010.

Mozurkewich, M.: The dissociation constant of ammonium nitrate and its dependence on temperature, relative humidity and particle size,
605 Atmospheric Environment. Part A. General Topics, 27, 261–270, 1993.

Murray, L. T.: Lightning NO x and impacts on air quality, Current Pollution Reports, 2, 115–133, 2016.

Ordóñez, C., Garrido-Perez, J. M., and García-Herrera, R.: Early spring near-surface ozone in Europe during the COVID-19 shutdown: Meteorological effects outweigh emission changes, Science of the total environment, 747, 141 322, 2020.

Pathakoti, M., Muppalla, A., Hazra, S., Dangeti, M., Shekhar, R., Jella, S., Mullapudi, S. S., Andugulapati, P., and Vijayasundaram, U.: An
610 assessment of the impact of a nation-wide lockdown on air pollution–a remote sensing perspective over India, Atmospheric Chemistry and Physics Discussions, pp. 1–16, 2020.

Pay, M. T., Jiménez-Guerrero, P., and Baldasano, J. M.: Assessing sensitivity regimes of secondary inorganic aerosol formation in Europe with the CALIOPE-EU modeling system, Atmospheric Environment, 51, 146–164, 2012.

Petetin, H., Sciare, J., Bressi, M., Gros, V., Rosso, A., Sanchez, O., Sarda-Estève, R., Petit, J.-E., and Beekmann, M.: Assessing the ammo-
615 nium nitrate formation regime in the Paris megacity and its representation in the CHIMERE model, Atmospheric Chemistry and Physics, 16, 10 419–10 440, 2016.

Petetin, H., Bowdalo, D., Soret, A., Guevara, M., Jorba, O., Serradell, K., and Pérez García-Pando, C.: Meteorology-normalized impact of the COVID-19 lockdown upon NO 2 pollution in Spain, Atmospheric Chemistry and Physics, 20, 11 119–11 141, 2020.

Putaud, J.-P., Pozzoli, L., Pisoni, E., Martins Dos Santos, S., Lagler, F., Lanzani, G., Dal Santo, U., and Colette, A.: Impacts of the COVID-19
620 lockdown on air pollution at regional and urban background sites in northern Italy, Atmospheric Chemistry and Physics, 21, 7597–7609, 2021.

Qu, Z., Jacob, D. J., Silvern, R. F., Shah, V., Campbell, P. C., Valin, L. C., and Murray, L. T.: US COVID-19 shutdown demonstrates impor-tance of background NO2 in inferring NOx emissions from satellite NO2 observations, Geophysical research letters, 48, e2021GL092 783, 2021.

625 Ramanantenasoa, M. M. J., Gilliot, J.-M., Mignolet, C., Bedos, C., Mathias, E., Eglin, T., Makowski, D., and Génermont, S.: A new frame-work to estimate spatio-temporal ammonia emissions due to nitrogen fertilization in France, Science of the Total Environment, 645, 205–219, 2018.

Renner, E. and Wolke, R.: Modelling the formation and atmospheric transport of secondary inorganic aerosols with special attention to regions with high ammonia emissions, Atmospheric Environment, 44, 1904–1912, 2010.

630 Russell, A. G., Cass, G. R., and Seinfeld, J. H.: On some aspects of nighttime atmospheric chemistry, Environmental science & technology, 20, 1167–1172, 1986.

Salameh, D., Detournay, A., Pey, J., Pérez, N., Liguori, F., Saraga, D., Bove, M. C., Brotto, P., Cassola, F., Massabò, D., et al.: PM2. 5 chemical composition in five European Mediterranean cities: a 1-year study, Atmospheric Research, 155, 102–117, 2015.

Samek, L., Stegowski, Z., Styszko, K., Furman, L., Zimnoch, M., Skiba, A., Kistler, M., Kasper-Giebl, A., Rozanski, K., and Konduracka,
635 E.: Seasonal variations of chemical composition of PM2. 5 fraction in the urban area of Krakow, Poland: PMF source attribution, Air Quality, Atmosphere & Health, 13, 89–96, 2020.

Scarlat, N., Fahl, F., Dallemand, J.-F., Monforti, F., and Motola, V.: A spatial analysis of biogas potential from manure in Europe, Renewable and Sustainable Energy Reviews, 94, 915–930, 2018.

Schaap, M., Loon, M. v., Ten Brink, H., Dentener, F., and Builtjes, P.: Secondary inorganic aerosol simulations for Europe with special
640 attention to nitrate, Atmospheric Chemistry and Physics, 4, 857–874, 2004.

Schiferl, L. D., Heald, C. L., Damme, M. V., Clarisse, L., Clerbaux, C., Coheur, P.-F., Nowak, J. B., Neuman, J. A., Herndon, S. C., Roscioli, J. R., et al.: Interannual variability of ammonia concentrations over the United States: sources and implications, Atmospheric Chemistry and Physics, 16, 12 305–12 328, 2016.

Schumann, U., Poll, I., Teoh, R., Koelle, R., Spinielli, E., Molloy, J., Koudis, G. S., Baumann, R., Bugliaro, L., Stettler, M., et al.: Air traffic
645 and contrail changes over Europe during COVID-19: a model study, Atmospheric Chemistry and Physics, 21, 7429–7450, 2021.

Seinfeld, J. H. and Pankow, J. F.: Organic atmospheric particulate material, Annual review of physical chemistry, 54, 121–140, 2003.

Shah, V., Jaeglé, L., Thornton, J. A., Lopez-Hilfiker, F. D., Lee, B. H., Schroder, J. C., Campuzano-Jost, P., Jimenez, J. L., Guo, H., Sullivan, A. P., et al.: Chemical feedbacks weaken the wintertime response of particulate sulfate and nitrate to emissions reductions over the eastern United States, Proceedings of the National Academy of Sciences, 115, 8110–8115, 2018.

650 Shah, V., Jacob, D. J., Li, K., Silvern, R. F., Zhai, S., Liu, M., Lin, J., and Zhang, Q.: Effect of changing NO x lifetime on the seasonality and long-term trends of satellite-observed tropospheric NO 2 columns over China, Atmospheric Chemistry and Physics, 20, 1483–1495, 2020.

Sharma, M., Kishore, S., Tripathi, S., and Behera, S.: Role of atmospheric ammonia in the formation of inorganic secondary particulate matter: a study at Kanpur, India, Journal of Atmospheric Chemistry, 58, 1–17, 2007.

655 Sillman, S.: The relation between ozone, NOx and hydrocarbons in urban and polluted rural environments, Atmospheric Environment, 33, 1821–1845, 1999.

Sillman, S., Logan, J. A., and Wofsy, S. C.: The sensitivity of ozone to nitrogen oxides and hydrocarbons in regional ozone episodes, Journal of Geophysical Research: Atmospheres, 95, 1837–1851, 1990.

Solberg, S., Walker, S.-E., Schneider, P., and Guerreiro, C.: Quantifying the Impact of the Covid-19 Lockdown Measures on Nitrogen Dioxide
660 Levels throughout Europe, Atmosphere, 12, 131, 2021.

Souri, A. H., Chance, K., Bak, J., Nowlan, C. R., González Abad, G., Jung, Y., Wong, D. C., Mao, J., and Liu, X.: Unraveling Pathways of Elevated Ozone Induced by the 2020 Lockdown in Europe by an Observationally Constrained Regional Model: Non-Linear Joint Inversion of NO x and VOC Emissions using TROPOMI, Atmospheric Chemistry and Physics Discussions, pp. 1–45, 2021.

Squizzato, S., Masiol, M., Brunelli, A., Pistollato, S., Tarabotti, E., Rampazzo, G., and Pavoni, B.: Factors determining the formation of
665 secondary inorganic aerosol: a case study in the Po Valley (Italy), Atmospheric chemistry and physics, 13, 1927–1939, 2013.

Steinfeld, J. I.: Atmospheric chemistry and physics: from air pollution to climate change, Environment: Science and Policy for Sustainable Development, 40, 26–26, 1998.

Steinmetz, H., Batzdorfer, V., and Bosnjak, M.: The ZPID lockdown measures dataset for Germany, 2020.

Stephens, S., Madronich, S., Wu, F., Olson, J., Ramos, R., Retama, A., and Munoz, R.: Weekly patterns of México City's surface concentrations of CO, NO x, PM 10 and O 3 during 1986–2007, Atmospheric Chemistry and Physics, 8, 5313–5325, 2008.

Tai, A. P., Mickley, L. J., and Jacob, D. J.: Impact of 2000–2050 climate change on fine particulate matter ($PM_{2.5}$) air quality inferred from a multi-model analysis of meteorological modes, Atmospheric chemistry and physics, 12, 11 329–11 337, 2012.

Theys, N., Smedt, I. D., Yu, H., Danckaert, T., Gent, J. v., Hörmann, C., Wagner, T., Hedelt, P., Bauer, H., Romahn, F., et al.: Sulfur dioxide retrievals from TROPOMI onboard Sentinel-5 Precursor: algorithm theoretical basis, Atmospheric Measurement Techniques, 10, 119–153, 2017.

Turner, A. J., Kim, J., Fitzmaurice, H., Newman, C., Worthington, K., Chan, K., Wooldridge, P. J., Köehler, P., Frankenberg, C., and Cohen, R. C.: Observed Impacts of COVID-19 on Urban CO 2 Emissions, Geophysical Research Letters, 47, e2020GL090 037, 2020.

Viatte, C., Wang, T., Damme, M. V., Dammers, E., Meleux, F., Clarisse, L., Shephard, M. W., Whitburn, S., Coheur, P. F., Cady-Pereira, K. E., et al.: Atmospheric ammonia variability and link with particulate matter formation: a case study over the Paris area, Atmospheric Chemistry and Physics, 20, 577–596, 2020.

Viatte, C., Petit, J.-E., Yamanouchi, S., Van Damme, M., Doucerain, C., Germain-Piaulenne, E., Gros, V., Favez, O., Clarisse, L., Coheur, P.-F., et al.: Ammonia and PM2. 5 Air Pollution in Paris during the 2020 COVID Lockdown, Atmosphere, 12, 160, 2021.

Von Schneidemesser, E., Monks, P. S., and Plass-Duelmer, C.: Global comparison of VOC and CO observations in urban areas, Atmospheric Environment, 44, 5053–5064, 2010.

Wang, L., Wang, J., and Fang, C.: Assessing the Impact of Lockdown on Atmospheric Ozone Pollution Amid the First Half of 2020 in Shenyang, China, International Journal of Environmental Research and Public Health, 17, 9004, 2020.

Wang, S., Nan, J., Shi, C., Fu, Q., Gao, S., Wang, D., Cui, H., Saiz-Lopez, A., and Zhou, B.: Atmospheric ammonia and its impacts on regional air quality over the megacity of Shanghai, China, Scientific reports, 5, 1–13, 2015.

Wang, W., van der A, R., Ding, J., van Weele, M., and Cheng, T.: Spatial and temporal changes of the ozone sensitivity in China based on satellite and ground-based observations, Atmospheric Chemistry and Physics, 21, 7253–7269, 2021.

Wang, Y., Zhang, Q., He, K., Zhang, Q., and Chai, L.: Sulfate-nitrate-ammonium aerosols over China: response to 2000–2015 emission changes of sulfur dioxide, nitrogen oxides, and ammonia, Atmospheric Chemistry and Physics, 13, 2635–2652, 2013.

Watson, J. G., Chow, J. C., Lurmann, F. W., and Musarra, S. P.: Ammonium nitrate, nitric acid, and ammonia equilibrium in wintertime Phoenix, Arizona, Air & Waste, 44, 405–412, 1994.

Webb, J., Menzi, H., Pain, B., Misselbrook, T., Dämmgen, U., Hendriks, H., and Döhler, H.: Managing ammonia emissions from livestock production in Europe, Environmental pollution, 135, 399–406, 2005.

Werf, G. R., Randerson, J. T., Giglio, L., Leeuwen, T. T. v., Chen, Y., Rogers, B. M., Mu, M., Van Marle, M. J., Morton, D. C., Collatz, G. J., et al.: Global fire emissions estimates during 1997–2016, Earth System Science Data, 9, 697–720, 2017.

Womack, C., McDuffie, E., Edwards, P., Bares, R., de Gouw, J., Docherty, K., Dubé, W., Fibiger, D., Franchin, A., Gilman, J., et al.: An odd oxygen framework for wintertime ammonium nitrate aerosol pollution in urban areas: NOx and VOC control as mitigation strategies, Geophysical Research Letters, 46, 4971–4979, 2019.

Wu, S.-Y., Hu, J.-L., Zhang, Y., and Aneja, V. P.: Modeling atmospheric transport and fate of ammonia in North Carolina—Part II: Effect of ammonia emissions on fine particulate matter formation, Atmospheric Environment, 42, 3437–3451, 2008.

Wu, Y., Gu, B., Erisman, J. W., Reis, S., Fang, Y., Lu, X., and Zhang, X.: PM2. 5 pollution is substantially affected by ammonia emissions in China, Environmental Pollution, 218, 86–94, 2016.

Yan, C., Tham, Y. J., Zha, Q., Wang, X., Xue, L., Dai, J., Wang, Z., and Wang, T.: Fast heterogeneous loss of N2O5 leads to significant night-time NOx removal and nitrate aerosol formation at a coastal background environment of southern China, Science of the Total Environment, 677, 637–647, 2019.

Yarwood, G., Stoeckenius, T. E., Heiken, J. G., and Dunker, A. M.: Modeling weekday/weekend ozone differences in the Los Angeles region for 1997, Journal of the Air & Waste Management Association, 53, 864–875, 2003.

Yin, H., Lu, X., Sun, Y., Li, K., Gao, M., Zheng, B., and Liu, C.: Unprecedented decline in summertime surface ozone over eastern China in 2020 comparably attributable to anthropogenic emission reductions and meteorology, Environmental Research Letters, 2021.

Zhai, S., Jacob, D. J., Wang, X., Liu, Z., Wen, T., Shah, V., Li, K., Moch, J. M., Bates, K. H., Song, S., et al.: Control of particulate nitrate air pollution in China, Nature Geoscience, pp. 1–7, 2021.

Zhang, R., Wang, G., Guo, S., Zamora, M. L., Ying, Q., Lin, Y., Wang, W., Hu, M., and Wang, Y.: Formation of urban fine particulate matter, Chemical reviews, 115, 3803–3855, 2015.